INFORMATION TO USERS

This manuscript has been reproduced from the microfilm master. UMI films the text directly from the original or copy submitted. Thus, some thesis and dissertation copies are in typewriter face, while others may be from any type of computer printer.

The quality of this reproduction is dependent upon the quality of the copy submitted. Broken or indistinct print, colored or poor quality illustrations and photographs, print bleedthrough, substandard margins, and improper alignment can adversely affect reproduction.

In the unlikely event that the author did not send UMI a complete manuscript and there are missing pages, these will be noted. Also, if unauthorized copyright material had to be removed, a note will indicate the deletion.

Oversize materials (e.g., maps, drawings, charts) are reproduced by sectioning the original, beginning at the upper left-hand corner and continuing from left to right in equal sections with small overlaps.

ProQuest Information and Learning
300 North Zeeb Road, Ann Arbor, MI 48106-1346 USA
800-521-0600

FLUORESCENCE INVESTIGATIONS OF THE SUPRAMOLECULAR HOST-GUEST INCLUSION COMPLEXES OF CUCURBIT[7]URIL AND SULFONIC CALIXARENES

A Thesis

Submitted to the Graduate Faculty

in Partial Fulfilment of the Requirements

for the Degree of

Master of Science

in the Department of Chemistry

Faculty of Science

University of Prince Edward Island

© Natasa Stojanovic

Charlottetown, P.E.I.

April 2002

SIGNATURE PAGES

ii-iii

REMOVED

ABSTRACT

In this project, fluorescence spectroscopy was used to study the supramolecular host properties of cucurbit[7]uril (CB[7]) and water soluble sulfonic calixarenes and to identify the useful properties of these compounds as potential supramolecular hosts.

The significant enhancement of the fluorescence of 2,6-ANS by CB[7], by a factor of 25, was observed in both potassium phosphate buffer and 0.2 M Na_2SO_4 solutions. The excellent fit of the enhancement as a function of CB[7] concentration data in both solvents indicate that simple 1:1 complexation is occurring between the 2,6-ANS guest and CB[7] host, with binding constants of 490 ± 80 M^{-1} and 244 ± 98 M^{-1} , in potassium phosphate buffer and 0.2 M Na_2SO_4, respectively. The lack of spectral shift indicates that only the phenyl ring of 2,6-ANS is included in the cavity. Results suggest that a much stronger complex is formed between 2,6-ANS and CB[7] as compared with CB[6]. Thus, the larger cavity and portal (7.3 Å and 5.4 Å, respectively) of CB[7], makes it a much better size match and host for the 2,6-ANS phenyl ring than CB[6] with the cavity and portals of 5.8 Å and 3.9 Å, respectively, resulting in a much larger fluorescence enhancement as well as in a much stronger inclusion complex. Thus, CB[7] is seen to have significantly improved host properties over the original cucurbituril,CB[6], as a result of its more spacious internal cavity.

The results obtained by studying the complexation of 1,8-ANS with CB[7] are very different from those with 2,6-ANS. The maximum fluorescence enhancement of 120 is much larger than that of 25 observed for 2,6-ANS. Also, significant blue shifting of the

1,8-ANS spectrum by 48 nm is observed, while for 2,6-ANS observed blue shift is only 7 nm. Results clearly indicate the formation of the higher-order inclusion complexes than the simple 1:1 complexes indicated for 2,6-ANS, and indicate the inclusion of the naphthalene ring into the CB[7] cavity. Polarity studies showed that cavity of CB[7] is relatively nonpolar with the cavity polarity similar to 50:50 (Vol./Vol.) methanol:ethanol mixture.

The van't Hoff plot of lnK versus 1/T for the complexation of 2,6-ANS with CB[7] is strongly curved, meaning that ΔH and ΔS for inclusion are not independent of T, even over the relatively small temperature range used. The curvature in the van't Hoff plot indicates that there is a change in the total heat capacity, ΔCp, for the inclusion process, i.e. Cp of the complex is different from the total Cp of the free guest and host. [7] In other words, there is non-zero ΔCp for this inclusion process, unlike the case of most inclusion phenomena reported in the literature.

The time-resolved fluorescence studies showed that the fluorescence decay curve of the inclusion complexes of 2,6-ANS molecule is best described by a two-exponential fit decay, indicating that at least two different types of 1:1 complexes exist, and illustrating that these host-guest inclusion systems are heterogeneous.

In the case of complexation by water-soluble sulfonic calixarenes, each probe used in this project showed decreased fluorescence upon addition of the calixarene of interest, whereas inclusion of the probe within the less polar calixarene cavity would be expected to result in fluorescence enhancement. The phenomenon (decreased fluorescence) observed by studying the inclusion complexes of water soluble sulfonic

calixarenes with different probes could be a result of conformation properties, functionalization of aromatic rings, π-π interactions between the aromatic guest and the phenolic ring of the calixarene, and the complexity of the calixarene structure.

Acknowledgments

Most importantly, I would like to thank my supervisor Dr. Brian Wagner whose great help, endless patience, and knowledge were greatly appreciated. His dedication to research was truly an inspiration. This project would not have been such a success without his help and understanding. I also would like to thank him for four wonderful years in his research lab, specially for the last two while working on my project. A simple "thank you" can not express my appreciation for teaching me how to think, understand, appreciate and apply important principles of science. THANK YOU.

I would also like to thank Greg Mc Manus for being a such wonderful lab friend and colleague as well as for sharing all frustrations and achievements with me.

I would like thank all faculty members of the UPEI Chemistry Department for their generous assistances. An specially great thanks to Dr. Nola Etkin for her help on the procedure for purification of the impure calixarenes. Also, I would like to thank Dawna Lund and Sharon Martin.

Table of Contents

List of Figures x

List of Tables xi

I. *INTRODUCTION* 1
- I.1 *Supramolecular Chemistry* 4
- I.2 *Fluorescence Spectroscopy* 17
- I.3 *Thermodynamic Considerations* 15
- I.4 *Host Molecules Studied* 16
- I.4.1 *Cucurbit[n]urils* 16
- I.4.2 *p-Sulfonic Calix[n]arenes* 19
- I.5 *Fluorescent Guest Molecules Used* 23

II. *EXPERIMENTAL* 27
- II.1 *Chemical Sources* 27
- II.2 *Sample Preparation* 28
- II.2.1 *Cucurbit[7]uril Sample Preparation* 28
- II.2.2 *p-Sulfonic Calix[n]arenes Sample Preparation* 29
- II.3 *Absorption Studies* 31
- II.4 *Steady-State Fluorescence* 32
- II.5 *Determination of Association Constants (K)* 34
- II.6 *Temperature Studies* 36
- II.7 *Time Resolved Fluorescence* 36

III. *INCLUSION COMPLEXES OF CUCURBIT[7]URIL* 39
- III.1 *Fluorescence Enhancement Studies* 39
- III.1.1 *2,6-ANS Results in Potassium Phosphate Buffer and 0.2M Na_2SO_4* 39
- III.1.2 *1,8-ANS Results in Potassium Phosphate Buffer and 0.2M Na_2SO_4* 44
- III.1.3 *Discussion* 48
- III.2 *Cavity Polarity of CB[7]* 55
- III.3 *Thermodynamics* 62
- III.4 *Time-resolved Fluorescence Results* 68

(*Continued*)

IV. *INCLUSION COMPLEXES OF CALIXARENES* 78
IV.1 *ANS as Guest* 79
IV.2 *Dansyl Lysine as Guest* 80
IV.3 *Nile Red as Guest* 84
IV.4 *Lanthanides as Guests* 85
IV.5 *Other Probes as Guests* 88
IV.6 *Fluorescence Studies of Calixarene Inclusion Complexes in the Literature* 88
IV.7 *Discussion* 90

V. *CONCLUSIONS* 95

VI. *REFERENCES* 99

List of Figures

Figure 1. *Molecular Structure of Cucurbituril* 2
Figure 2. *Molecular Structure of Calixarenes* 3
Figure 3. *Formation of a 1:1 Host-Guest Complex* 5
Figure 4. *Jablonski Diagram* 9
Figure 5. *Polarity Effect on Energy Gap* 13
Figure 6. *Molecular Structure Cucurbit[7]uril* 18
Figure 7. *Molecular structures of p-sulfonatocalix[4]arene ($R=SO_3^-$)* 20
Figure 8. *Molecular Structures of 1,8-ANS and 2,6 ANS* 24
Figure 9. *Molecular structures of* ***1*** *Nile Blue,* ***2*** *Dansyl Lysine,* ***3*** *Nile Red,* ***4*** *Neutral Red, and* ***5*** *Resorufin.* 25
Figure 10. *Fluorescence spectra of 2,6-ANS in the presence of various amounts of CB[7]*: 1 *0 mM;* 2 *2 mM*; 3 6 mM; 4 *10 mM.* 40
Figure 11. *The fluorescence enhancement of, F/F_0, of 2,6-ANS in potassium phosphate buffer as a function of CB[7] concentration* 42
Figure 12. *Reciprocal plot of $1/(F_0/F - 1)$ vs. 1/[CB[7]] for 2,6-ANS* 43
Figure 13. *Fluorescence spectra of 1,8-ANS in the presence of various amounts of CB[7] in potassium phosphate buffer*:1 *0 mM;* 2 *2 mM*; 3 6 mM; 4 *10 mM.* 45
Figure 14. *The fluorescence enhancement of, F/F_0, of 1,8-ANS in potassium phosphate buffer as a function of CB[7] concentration* 46
Figure 15. *Reciprocal plot of $F_0/F - 1$ vs. 1/[CB[7]] for 1,8-ANS* 47
Figure 16. *Axial and equatorial inclusion of 2,6-ANS molecule within the host cavity* 54
Figure 17. *Normalized fluorescence spectra of 2,6-ANS in H_2O buffer (__.), methanol (...), ethanol (----), and in 10 mM CB[7] (___).* 56
Figure 18. *Normalized fluorescence spectra of 1,8-ANS in H_2O buffer (__.), methanol (...), ethanol (----), and in 10 mM CB[7] (___).* 57
Figure 19. *Plot of fluorescence maximum $\nu_{F,max}$ vs. dielectric constant, ε, for 1,8-ANS in various solvents and aqueous CB[7] solution.* 61
Figure 20. *Plot of lnK vs. 1/T for CB[7]:2,6-ANS complex* 63
Figure 21. *Plot of A_2/A_1 plotted as a function of CB[7] for 2,6-ANS.* 71
Figure 22. *Plot of τ/τ_0 plotted as a function of CB[7] for 2,6-ANS.* 73
Figure 23. *Fluorescence decay curve of 2,6-ANS with 10mM CB[7].* 76
Figure 24. *Absorbance spectra of Dansyl Lysine with p-sulfonic calix[4]arene in water solution* 82
Figure 25. *Fluorescence spectra of Eu(III) and p-sulfonic calix[4]arene crystals* 87

List of Tables

Table 1: *List of chemicals used for this project* 28
Table 2. *Solvent polarity parameters and absorption and emission maxima of 1,8-ANS in various solvents* 59
Table 3. *Association constants at various temperatures for CB[7]:2,6-ANS complex* 62
Table 4. *Lifetime data for 2,6-ANS with various concentrations of CB[7].* 70
Table 5. *Absorbance and fluorescence parameters of 2,6-ANS with 4SCA and 6SCA in water* 79
Table 6. *Absorbance and fluorescence parameters of dansyl lysine with and without 4SCA in water* 81
Table 7. *Absorbance parameters of DL/4SCA and 4SCA in H_2O by different [4SCA]* 83

I. *INTRODUCTION*

The main interest of this project is the investigation of the physical and spectroscopic properties of some particular host-guest inclusion complexes. Host-guest inclusion can be defined as the phenomenon in which a small guest molecule becomes incorporated inside the cavity of larger, cage-like host molecule. The binding between the host and guest is relatively weak, consisting in general of intermolecular forces, including van der Waals forces and hydrogen bonding. Thus, there is an equilibrium established between the complex and the free host and guest molecules. The specific systems of interest in this project are those involving two specific types of host molecules, namely cucurbiturils and water soluble calixarenes, with a wide variety of fluorescent probes (fluorophores) as guest molecules.

Cucurbituril, shown in Figure 1, is an interesting host molecule, which was first prepared in 1905 but not characterized until 1981.[1-3] Compared with other macrocyclic ligands, such as cyclodextrins, there have been few studies of the complexation behaviour of cucurbuturil. It forms stable host-guest complexes with small molecules. Recently, the synthesis of new cucurbituril homologues, cucurbit[n]urils, with n=5, 7, and 8 (n=6 is the original cucurbituril) have opened up new opportunities to expand the host-guest chemistry of cucurbiturils.[4] Studies with cucurbiturils so far have been very fruitful, both in providing an opportunity for systematic investigation of the thermodynamic and kinetic aspects of molecular recognition, and as a model for enzymic reactions. The extreme rigidity of the polycyclic cage structure of cucurbituril represents its most exceptional characteristic. This confers high selectivity among potential guests, allowing quantitative analysis of hydrophobic

and other binding phenomena. The availability of the various homologues with differing cavity sizes further adds to the importance and applicability of these hosts. This will be discussed in more detail in section 1.4.1.

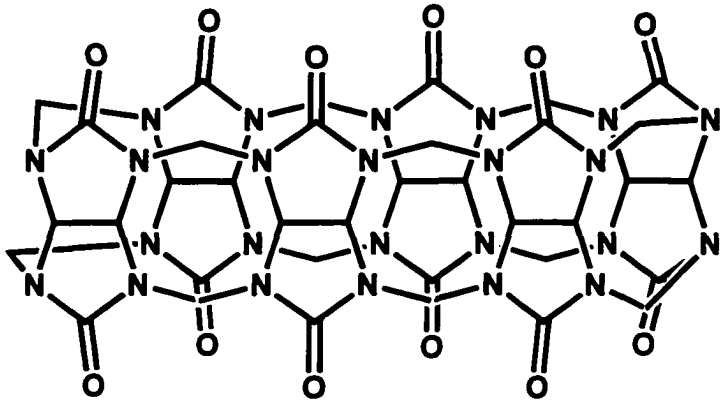

Cucurbit[6]uril

Figure 1. *Molecular structure of cucurbituril.*

Calixarenes are a group of phenolic macrocycles that have become significant in supramolecular chemistry only during the past decade. These compounds are cylinder-shaped with various cavity sizes and can form a variety of host-guest inclusion complexes. The shape and size of calixarenes (Figure 2) depend on the number of phenolic units, n, and on the type of substituent on the aromatic rings, R (upper rim), and at the phenolic oxygen atoms, R' (lower rim, R'=H in Figure 2). Thus, calixarenes are particularly attractive for

systematic studies of inclusion phenomena as a function of these parameters. There are many advantages to using calixarenes as host molecules because of their unique properties. The weak forces which play a major role in complex formation include hydrogen bonding, π-π interactions, electrostatic interactions, and dipole-dipole interactions. Calixarenes provide all of those characteristics. In spite of the diversity of calixarene structures available, the literature contains only a limited number of reports describing well-characterized complexation by calixarene hosts in the solution phase.

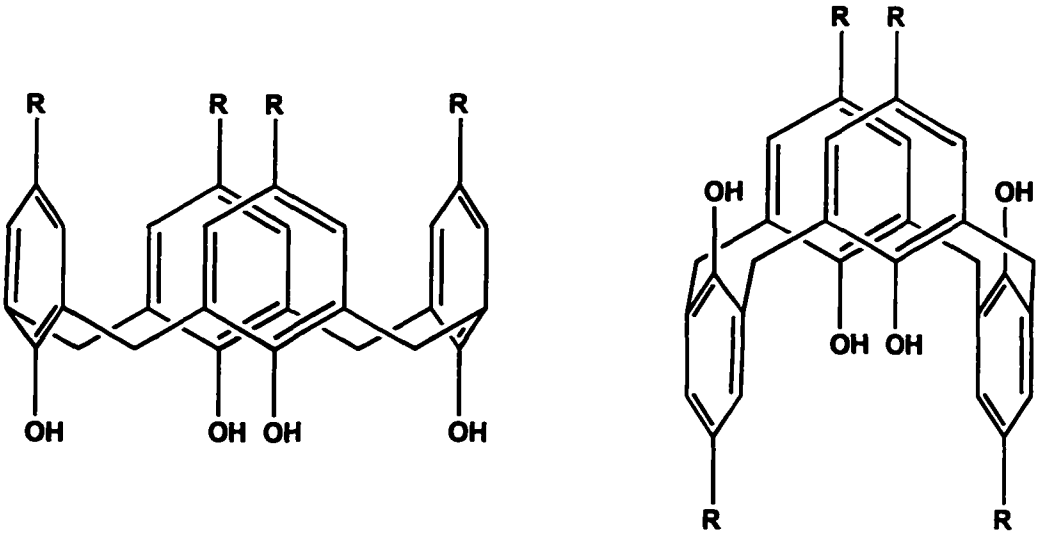

Figure 2. *Molecular structure of calixarenes.*

In this project, fluorescence spectroscopy was used to study the supramolecular host properties of both of the above mentioned types of host molecules, and to identify the useful properties of these compounds as potential supramolecular hosts.

I.1 *Supramolecular Chemistry*

Supramolecular chemistry is a field of science investigating various features of chemical species of a greater complexity than molecules themselves, that are held together and organized by means of intermolecular interactions. Therefore, supramolecular chemistry can be defined as "chemistry beyond molecule", where two or more chemical species are held together not by covalent bonds, but only by intermolecular forces.[5] These intermolecular forces are non-covalent bonds which include electrostatic interactions, van der Waals forces, hydrogen bonding, and hydrophobic effects. Electrostatic interactions (ion-ion, ion-dipole, and dipole-dipole) are attractions between opposite charges. Van der Waals forces, such as dispersion forces and dipole-dipole interactions, are attractive forces between molecules that occur when temporary dipoles of each molecule interact favourably. Hydrogen bonding consists of an attractive force existing between a hydrogen atom covalently bonded to an electronegative atom (e.g. fluorine, oxygen or nitrogen) and a second electronegative atom. The most important contributions to the complexation in aqueous solution are believed to originate from the hydrophobic effect, i.e. the penetration of the hydrophobic part of the guest molecule into the host cavity. A combination of these kinds of forces provides the enthalpic stabilization for the incorporation of the guest molecule within the host cavity,[5] and the stronger these forces are, the stronger will be the supramolecular complex. The simplest example of a supramolecular structure is a 1:1 host-guest inclusion complex, in which a smaller "guest" molecule becomes included within the internal cavity of a larger, hollow, cage-like "host" molecule. Such a complex involves the

minimum of two molecules to be considered supramolecular. The formation of such a complex is illustrated in Figure 3. This figure emphasizes that the formation of host-guest inclusion complexes in solution involves an equilibrium between the complex and the free guest and host molecules. In this project, in order to study the host-guest interactions, and the physical and the spectroscopic properties of these supramolecular host-guest inclusion complexes, a steady-state fluorescence spectroscopy method is used. It allows for the measurements of the fluorescence spectrum of the guest in the absence and presence of the host, and from these the effect of complexation on the guest fluorescence can be determined. One possible result of formation of the supramolecular complex of the fluorescent probe within the host is enhancement of the fluorescence intensity of the incorporated probe, as illustrated in Figure 3. This fluorescence enhancement, which will be explained in detail later, is very easy to accurately measure as well as to relate to environmental changes of the fluorophore, and thus provides an excellent method for studying the host-guest complexes.

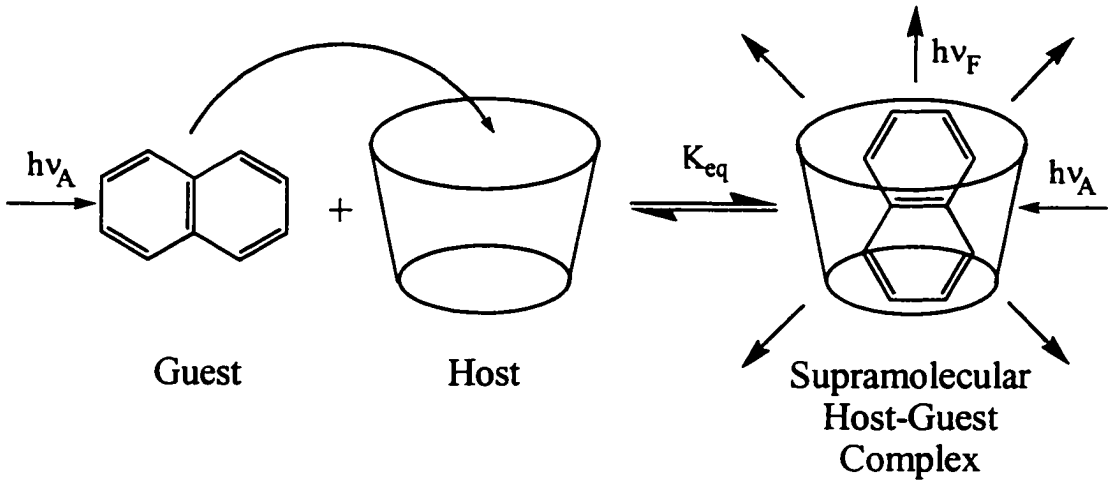

Figure 3. *Formation of a 1:1 host-guest complex.*

Figure 3 shows the formation of a 1:1 host:guest complex, in which one guest molecule resides inside the cavity of the host molecule. It is also possible that higher-order complexes can be formed. This includes a 2:1 complex, in which two hosts cap the ends of single guest molecule, a 1:2 complex in which two guests reside inside one host, or a 2:2 complex in which two hosts cap the ends of a pair face-to-face guests. The analysis of the fluorescence spectra of the probe molecule in the absence and presence of various amounts of the host enables both the determination of the complex stoichiometry as well as the determination of the association constants for complexation. These association binding constants (K) are very important parameters which provide significant information on how well the host molecule accommodates the guest molecule into its cavity. Furthermore, the temperature dependence of the complexation processes has also been studied, which allows for the determination of the two most fundamental thermodynamic quantities for the complexation process, the enthalpy and entropy. This provides for a better understanding of the forces responsible for the complexation of the guest molecule within the host.

Since the fluorescence lifetime is extremely sensitive to the guest environment, the investigation of the specific supramolecular host-guest systems by time-resolved spectroscopy can provide further useful insights into the interactions involved in host inclusion of a guest molecule. This is very useful since different host-guest complexes of the same stoichiometry can be formed as well as higher order complexes in concentrated host solutions. In contrast to steady-state fluorescence spectroscopy which measures the fluorescence intensity as a function of wavelength, time-resolved fluorescence measures fluorescence intensity as a function of time. Time-resolved fluorescence not only provides

information about the general environment of the fluorescent molecule, but also allows the kinetics of fluorescence to be studied.[6] During the course of this project, several host-guest complexes were studied using time-resolved fluorescence spectroscopy. The purpose of this part of the project was to determine the fluorescence lifetimes of the guest molecules upon complexation within the host as well as to obtain more information about the formation of these complexes, and to see whether the information obtained using the steady-state fluorescence could be obtained with this method as well.

I.2 *Fluorescence Spectroscopy*

Fluorescence spectroscopy involves the initial excitation of a probe molecule using light. The absorption of a photon by a probe molecule results in the promotion of an electron from an occupied bonding molecular orbital to an upper unoccupied orbital. There are two possibilities for this excited state: it will be a singlet if the two unpaired electrons have opposite spins; or it will be a triplet if the spins are parallel.[6] Soon after the promotion of the electron to the excited state, electronic deactivation occurs. If this deactivation, or decay, is accompanied by the excited molecule giving off a photon, it is referred to as an emission process. If during the emission process the electron undergoing the transition does not change its spin, the emission process is called *fluorescence*; on the other hand, if inversion of spin occurs, the emission process is called *phosphorescence*.[7] Fluorescence can be thus defined as the emission of a photon during the transition from an excited electronic state to a lower state, usually ground state, of the same multiplicity, while phosphorescence is the

emission which results from transition between the states of different multiplicity, generally triplet excited state returning to a singlet ground state.[7] Since spin inversion is a forbidden process, fluorescence is in general a much more favoured and common process than phosphorescence.

As can be seen from the Jablonski diagram presented in Figure 4, as soon as the molecule is excited from the ground state (S_0) to any vibrational level (v') of the excited state (S_1), vibrational relaxation usually occurs to the lowest vibrational level (v'=0) of the excited state. Vibrational relaxation is an extremely fast process which occurs on the picosecond time scale and therefore takes place before any emission has a chance to occur. Following the rapid vibrational relaxation the excited state can return to the ground state by two types of processes, radiative and non-radiative. The radiative process in this case is the already described fluorescence, in which the molecule returns to the ground state by releasing a photon. Since vibrational relaxation occurs prior to fluorescence emission, fluorescence will occur at a longer wavelength than absorption.[6]

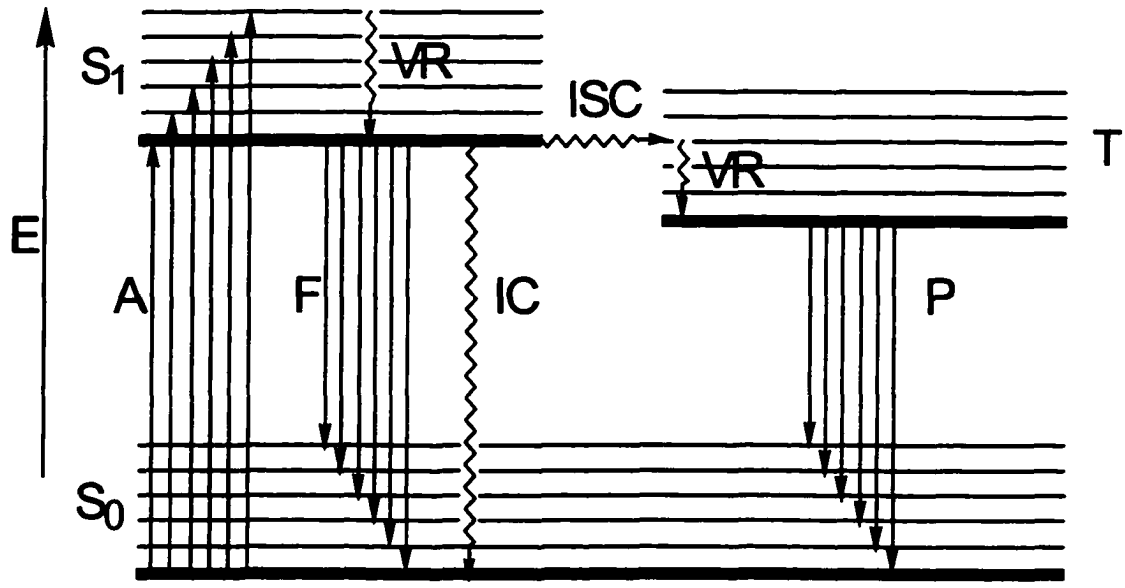

Figure 4. *Jablonski diagram.*

There are two possible non-radiative processes: internal conversion (IC) and intersystem crossing (ISC). Internal conversion is a horizontal, isoenergetic transition between vibrational levels of two states of the same multiplicity. It usually occurs from a low vibrational level of an excited electronic state to a high vibrational level (of the same energy) of a lower electronic state. This process is followed by vibrational relaxation to return the molecule to the ground state. Intersystem crossing involves a horizontal transition between a triplet and a singlet state. The electron changes spin and crosses to a vibrational level of the triplet state of the same energy. In these two types of processes the excited state energy is released as heat. Both of these processes compete with fluorescence; the intensity of

fluorescence thus depends upon the magnitude of the rate constant of radiative fluorescence process (k_F) relative to the total rate constants of all the decay processes, including the two non-radiative processes (k_{IC} and k_{ISC}).[7]

Kinetic analysis of the above mentioned and described radiative and non-radiative processes can provide the empirical formulas for two very important quantities of molecular fluorescence: the fluorescence lifetime and quantum yield. The fluorescence lifetime τ_F, is a measure of how long the fluorescence lasts, or it can be defined as the average period of time a fluorophore remains in the excited state.[8] In terms of reaction kinetics the fluorescence lifetime of a molecule can be defined in terms of the rate of depopulation of the first excited state after the excitation from the ground state.[9]

$$d[^1M^*]/dt = -[^1M^*]/\tau_F \qquad (1)$$

$$\text{or} \quad -d[^1M^*]/dt = (k_F + k_{IC} + k_{ISC})[^1M^*] \qquad (2)$$

Integrating this equation with respect to time gives the following simple monoexponential decay law.[9]

$$[^1M^*] = [^1M^*]_0 \, e^{-t/\tau_F} \qquad (3)$$

where $[^1M^*]$ and $[^1M^*]_0$ represent the excited state molar concentration at time t and t=0, respectively, and τ_F is the molecular fluorescence lifetime. Since fluorescence intensity, I_F, is given by the rate of fluorescence, $k_F [^1M^*]$, the fluorescence decay curve can be expressed

by the following equation:

$$I_F(t) = I_0 e^{-t/\tau_F} \qquad (4)$$

A plot of fluorescence intensity as a function of time gives a fluorescence decay curve, $I_F(t)$, which can be fitted by mathematical analysis to determine the lifetime τ_F, where

$$\tau_F = 1 / (k_F + k_{NR}) \qquad (5)$$

or

$$\tau_F = 1/ (k_F + k_{IC} + k_{ISC}) \qquad (6)$$

where k_F, k_{IC} and k_{ISC} represents radiative and non-radiative first-order rate constants.

The quantum yield indicates the efficiency of fluorescence. It represents the ratio of the number of molecules that fluoresce to the total number of excited molecules. The quantum yield of a molecule can be expressed as the ratio of the rate constant for the radiative emission to the total sum of the radiative and non-radiative processes:[11]

$$\phi_F = k_F/ (k_F + k_{IC} + k_{ISC}) = k_F/(k_F + k_{NR}) \qquad (7)$$

A high quantum yield will result in brighter fluorescence, *i.e.* a high fluorescence intensity. As can be seen from Equation (7), the quantum yield can be close to unity if the rates of non-radiative processes are much smaller than the rate of radiative decay. Internal conversion often competes strongly with fluorescence, therefore, the rate of internal conversion is important when studying the quantum yield of a molecule. If the two electronic states are close in energy, the rate of internal conversion will be large. This is because it is easier to have a high vibrational level of the lower excited state at the same energy as the upper excited state, thereby allowing internal conversion to occur. If this is the case, the quantum yield will decrease, resulting directly in a decrease in fluorescence intensity. This phenomenon can be defined by the Energy Gap Law, which provides the relationship between the rate of internal conversion, k_{IC}, and the energy difference between the S_0 and S_1, ΔE. This relationship is given by the following equation:

$$k_{IC} \alpha e^{-\Delta E/RT} \qquad (8)$$

In general, the excited state S_1 is more polar than the ground state, S_0, due to the promotion of an electron to the higher, larger, and more spread out molecular orbital. Therefore, the excited state molecule is more energetically stabilized relative to the ground state in a polar than in non polar solvent (environment). This greater stabilization of the excited state in polar solvent decreases the energy gap between the S_0 and S_1 states, and therefore, increases the rate of internal conversion. Transferring a molecule of interest from a polar to a non-polar solvent or environment, the reverse phenomenon will occur.

Destabilisation of the excited state will be observed, causing an increase in energy gap between the ground and excited states, as shown in Figure 5. This results in a decrease in k_{IC}, and thus an increase in quantum yield, ϕ_F, resulting in the observation of fluorescence enhancement.

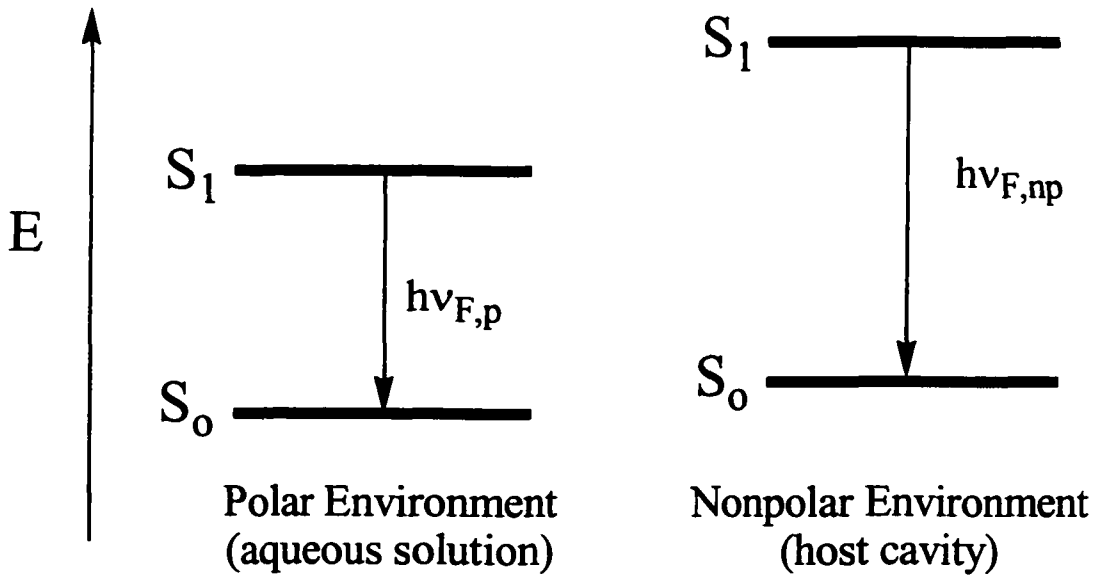

Figure 5. *Polarity effect on energy gap.*

The third very important property of molecular fluorescence is fluorescence wavelength maximum, $\lambda_{F,max}$, which indicates the difference in energy between the lowest vibrational level of excited state and the most probable vibrational level of the ground state. Therefore, the change in energy gap between the ground and excited state will affect both the emission wavelength maximum and quantum yield. An increase in energy gap ΔE will cause $\lambda_{F,max}$ to move to the shorter values of wavelength (higher energy) in the spectrum (blue-shift), since $\Delta E = hc/\lambda_F$. Furthermore, an increase in energy gap will decrease the rate of internal conversion (k_{IC}), which competes with the rate of the fluorescence emission. Therefore, this will result in an increase of the quantum yield.

For many probes the values of k_{IC} and k_{ISC} depend on the fluorophore's environment in a way determined by properties such as refractive index, temperature and the local polarity. In this project, the polarity of the environment of the fluorescent probe is changed upon inclusion within a host. Since many fluorescent probes are hydrophobic, polar aqueous solution is very unfavourable for them. However, if a host molecule that possesses a relatively non-polar cavity is added to the solution, the probe has the ability to incorporate itself within the cavity, allowing the same probe to experience a completely new, more favourable environment. This effect, of changing the fluorescence properties of a guest molecule by changing its local environment upon inclusion inside the host cavities, is main focus of this project and provides the means to study the supramolecular host-guest inclusion process. In most cases, fluorescence enhancement of the probe is observed upon inclusion. The measurement of this fluorescence enhancement as a function of added host concentration provides an accurate method for determining the value of the association

constant K for the inclusion process, as described in Chapter 2.

I.3 *Thermodynamic Considerations*

The thermodynamic properties of the host-guest inclusion process can be determined using a number of different techniques, including microcalorimetry, electronic absorption, potentiometric techniques, and fluorescence spectroscopy.[12] In this project fluorescence spectroscopy is the chosen method of study. Association (equilibrium) constants (K) are determined at various temperatures. These values can be used to determine the enthalpy change (ΔH^0) and entropy change (ΔS^0) of the inclusion process, using the following relationships:

$$\ln K = - \Delta G^0 / RT \qquad (9)$$

$$\Delta G^0 = \Delta H^0 - T \Delta S^0 \qquad (10)$$

Combination of Equations (9) and (10) gives the relationship between K, T, ΔH^0 and ΔS^0, which is known as the van't Hoff equation:

$$\ln K = -\Delta H^0/RT + \Delta S^0/R \qquad (11)$$

ΔS^0, the standard entropy change, is a measure of the change in disorder of the system, and ΔH^0, the standard enthalpy change, is a measure of the energy changes associated with the complexation.

Equation (11) shows that a plot of ln K against 1/T will have a slope equal to $-\Delta H^0/R$ and intercept equal to $\Delta S^0/R$. If the plot of ln K against 1/T is linear, this means that ΔH^0 and ΔS^0 are independent of temperature over the range investigated. The importance of the van't Hoff equation lies in the fact that from the plot of ln K against 1/T, the two thermodynamic quantities, enthalpy and entropy, can be determined giving further insight in to the host-guest complexation, and into which of the two dominates the formation of the supramolecular complexes.

I.4 *Host Molecules Studied*

In this project, the host molecules studied are cucurbiturils and water soluble calixarenes. Both of these host molecules possess hydrophobic cavities accessible to the different guest molecules, which make them of interest in this project.

I.4.1 *Cucurbit[n]urils*

The macrocyclic ligand cucurbituril was first synthesized by Behrend *et al.* in 1905.[1] The authors could not suggest any chemical structure for the reaction product at that time. It took more than 75 years before the chemical structure of this condensation product was determined and reported by Mock in 1981.[2,3] This interesting cage molecule is composed of six glucoluril units linked by methylene bridges, as was shown previously in Figure 1. It is a relatively rigid molecule possessing a cavity of ca. 5.5 Å in diameter, with two identical

portals of ca. 4 Å formed by carbonyl groups of the urea subunit.[2,13]

Similar to cyclodextrin, a much better known and more widely studied host molecule[14], the cavity can hold small organic molecules through hydrophobic interactions, but because of its structural rigidity as well as its polycyclic nature, it can not easily conform to the shape of the incorporated small probe molecules.[13] Also, unlike the cyclodextrins, the carbonyl groups at the portals allow molecules to bind through both charge-dipole and hydrogen-bonding interactions.[4] Recently, the preparation of cucurbituril homologues with 5 to 8 glycoluril monomers has been reported.[4] These are denoted as *cucurbit[n]urils* , and abbreviated in this work as CB[n], where n is the number of glycoluril monomers in the ring. For example, cucurbit[7]uril is shown in Figure 6. One of the most important properties of these new homologues is their high solubility in common solvents such as water and methanol. Another is the expanded cavities in the case of n=7 and n=8, yielding new hosts with potentially superior host abilities. Thus the synthesis of these higher CB homologues (CB[n], n= 7 and 8) with larger cavities, the dimensions of which are equivalent to those of β– and γ-CDs, respectively, opens up new possibilities in the chemistry of cucurbiturils as well as supramolecular chemistry itself.

Using NMR-techniques, Mock and co-workers investigated the complexation reaction between a large number of substituted ammonium ions as well as diammonium ions with the parent cucurbituril.[16,17] Bushman *et al.*[2,18] showed that the encapsulation ability of cucurbiturils can be extended to alkali and alkaline earth cations. He showed that ions can not only be incorporated within the cucurbituril cavity, but also they may interact with the carbonyl atoms at the portals, as was the case with these cations. In addition, Bushman and

co-workers have also reported association constants for the inclusions of alkali metal cations[1], alkaline earth cations[1,2], alkylamines[2], and alkyldiamines[2] within the CB[6] cavity.

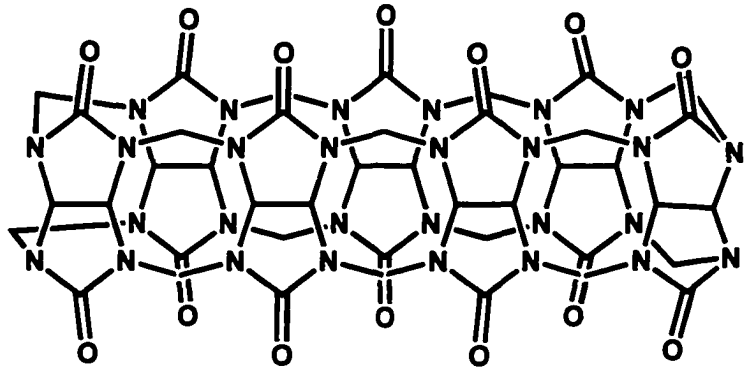

Cucurbit[7]uril

Figure 6. *Molecular structure cucurbit[7]uril.*

Cucurbituril has also been shown to form host-guest inclusion complexes with a wide range of neutral guest molecules in addition to ions, including amino acids and alcohols[3], tetrahydrofuran and different aromatic molecules[19]. All of these previous studies on the host-guest inclusion complexes of cucurbituril have been performed using NMR, UV-vis spectroscopy, or calorimetry. There have been relatively few studies of the effects of encapsulation of cucurbituril on the fluorescence of the incorporated guest molecule. The fluorescence studies of the host-guest inclusion complexes of the parent cucurbituril CB[6] in solution for the first time were reported by Wagner *et al.*[20]. In fact, none of the guest molecules previously encapsulated by cucurbituril had been shown to undergo fluorescence

enhancement upon incorporation within the CB cavity.[20]

Unlike the case of CB[6], there have been no experimental fluorescence studies of inclusion complexes of CB[7], or in fact any reported association constants for its inclusion complexes *via* any experimental techniques. In contrast, there have been some reports of inclusion abilities of CB[8] as host with macrocycles[21] and hetero charge transfer pairs [22], published by Kim and co-workers. In this project, the inclusion of several probes in CB[7] was studied using fluorescence spectroscopy. The observation of fluorescence enhancement of a guest molecule provides an excellent method for studying the as yet unknown inclusion abilities of CB[7], and may in addition lead to potential application of CB[7] as a molecular sensor for specific guests.[20] Thus, CB[7] will be the focus of a major portion of this project.

I.4.2 *p-Sulfonic Calix[n]arenes*

The second host molecules of interest studied in this project are water soluble calixarenes, *p*-sulfonic calix[4]arene and *p*-sulfonic calix[6]arene. Calixarenes are cyclic phenol oligomers linked by methylene groups.[23] These cylinder-shaped compounds with different cavity sizes can form a variety of host-guest type inclusion complexes. As can be seen from Figure 7, the shape and size of the calixarene depend on the number of phenolic units, n, and on the type of substituents on the aromatic nuclei, R, (upper rim), and phenolic oxygen (lower rim). All members of the series from n=4-14 are known. Recent applications of calixarenes include using them as accelerators for instant adhesives, stationary phases for

liquid chromatography, ion selective electrodes and ion scavengers for electronic devices.[24] They may also have applications in medical diagnostics and therapy. What makes calixarenes even more interesting is their ability to have numerous conformations, two of which are shown in Figure 7, the cone (left) and the 1,3-alternate (right). Therefore, compared to cyclodextrins in which the conformation is mostly immobilized, conformational freedom of calixarenes still remains.

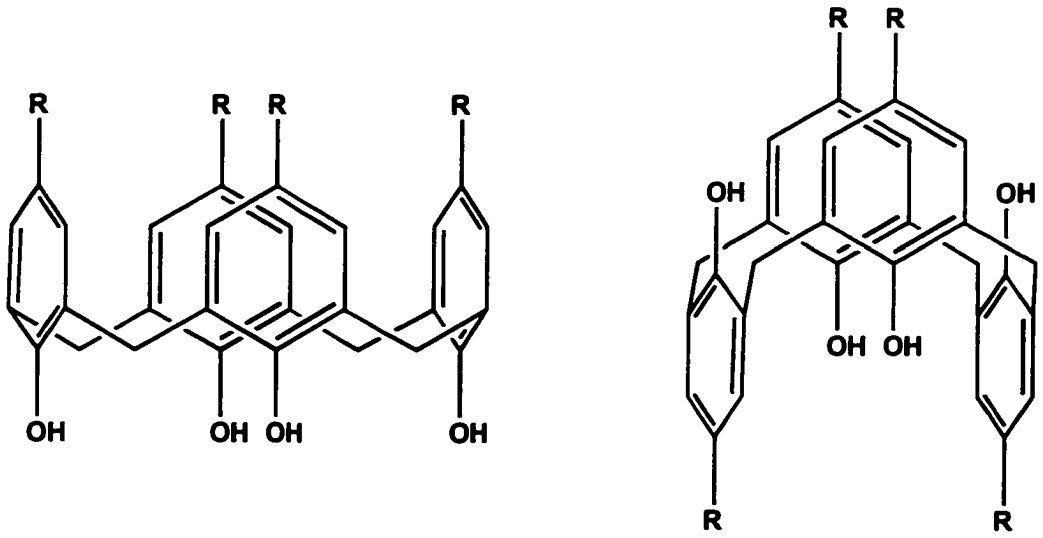

Figure 7. *Molecular structures of p-sulfonatocalix[4]arene ($R=SO_3^-$).*

The story of calixarenes as supramolecular hosts started in the beginning of the 19th century with the experiments of Adolf von Baeyer, continuing into the early part of the 20th century by the work of Leo Baekelend, and extending to the early 1940s with the experiments of Zinke and Niederl.[25] By this time it was not really clear what kind of

compound, or product was made. The investigation by Gutsche and co-workers, starting in mid 1970s, actually determined that the product made by the previous investigators, was a mixture of three different cyclic components, which are later introduced as calixarenes.[26] However, it was not until the end of the 1970s that the interest in calixarene chemistry raised, led by several groups, including the Mainz group of Kammerer, the Parma group of Andretti, Pochini and Ungaro, and the St. Louis group of Gutsche.[26] There have been extensive studies of the complexation abilities of calixarenes which indicate that their effectiveness as hosts is related on the absolute magnitude of their complexation constant[26], but also on their rather nonselective recognition towards guest molecules, due to their flexibility and conformational isomerism. Several inclusion complexes of neutral organic molecules with the parent calixarenes and their upper rim substituted analogues have been reported in literature. For example, it has been shown that *p-i*-propylcalix[4]arene forms a 1:1 supramolecular inclusion complex with p-xylene.[27] Also there are many other examples of host-guest complexation of other upper-rim substituted calixarenes with toluene, benzene and pyridine.[27] However, it is important to note that these examples involve only alkyl substituted calix[4]arene as host molecules. If alkyl groups are removed from the upper rim of the parent calix[4]arene their ability to form inclusion complexes with aromatic neutral molecules drops, and no such complexes have been observed so far.[27]There are also a number of examples of complexation between different metal ions, lanthanides, and organic cations with parent and substituted calixarenes.

The biggest disadvantage of the parent calixarene molecules is that they are insoluble in water, and generally have low solubilities in most organic solvents. Thus, for a very long

period of time, studies on the host-guest chemistry of calixarenes in solution have been limited. In fact, evidence supporting the formation of their inclusion complexes in solution came much later after the discovery of calixarenes. In order to find the evidence for a such phenomenon, as well as to promote hydrophobic effects as result of complexation, the parent calixarenes have been functionalised by polar groups, and thus water soluble calixarenes have been produced. The first water soluble calixarene was prepared by Ungaro and co-workers[28] by substituting the phenolic hydrogens by carboxymethyl groups. Most recently, Shinkai and co-workers[29] have obtained water soluble calixarenes by introducing sulfonic acid groups in the *p*-positions at the upper rim of the molecule. Besides sulfono-calixarene, several types of water soluble calixarenes have been synthesized as well, such as amino-[30,31], nitro-[32], carboxyl-[33], and phosphonato-calixarenes[34]. All of these types of water soluble calixarenes have enormous complexation abilities, and therefore, a number of different host-guest complexes by these calixarenes have now been reported. However, there have been relatively few studies of the effects of encapsulation of water soluble calixarenes on the fluorescence of the incorporated guest molecules. The only examples are those of Shinkai and co-workers, who reported fluorescence studies on inclusion complexes of sulfonic derivatives of calix[6]arene with aminonaphthalene derivatives[35] and pyrene[36] as fluorescent guests, and of phosphonato calixarenes with 1,8 ANS as fluorescent guest[34]. In other related work, Barra studied the association equilibrium constants and thermodynamic parameters (*i.e.* ΔH^0 and ΔS^0) for complexation between N,N-dimethylindoaniline[37] and *p*-sulfonated calix[n]arene (n=4,6 and 8) in aqueous solution using UV-Vis spectroscopy as the technique. Inclusion complexation of Auramine O Dye[23] and Acridine Red Dye[38] with

water soluble sulfonic calix[6] arene has also been reported.

Therefore, because of the unique properties of calixarenes, such as the hydrophobic cavity, and the weak forces which play a major role in complex formation, including hydrogen bonding, π-π interactions, electrostatic interactions, and dipole-dipole moments, there are many advantages to their use as host molecules. In this project, an investigation of the formation of host-guest inclusion complexes between *p*-sulfonic calix[4]arene and *p*-sulfonic calix[6]arene and several different fluorescent molecules has been carried out.

I.5 *Fluorescent Guest Molecules Used*

Guest probe molecules which are used in this project to study host-guest inclusion complexes with cucurbit[7]uril as host are two isomeric anilinonaphthalene sulfonate probes, 8-anilino-1-naphthalene-sulfonic acid (1,8-ANS) and 2-anilinonaphthalene-6-sulfonic acid (2,6 ANS), shown in Figure 8.

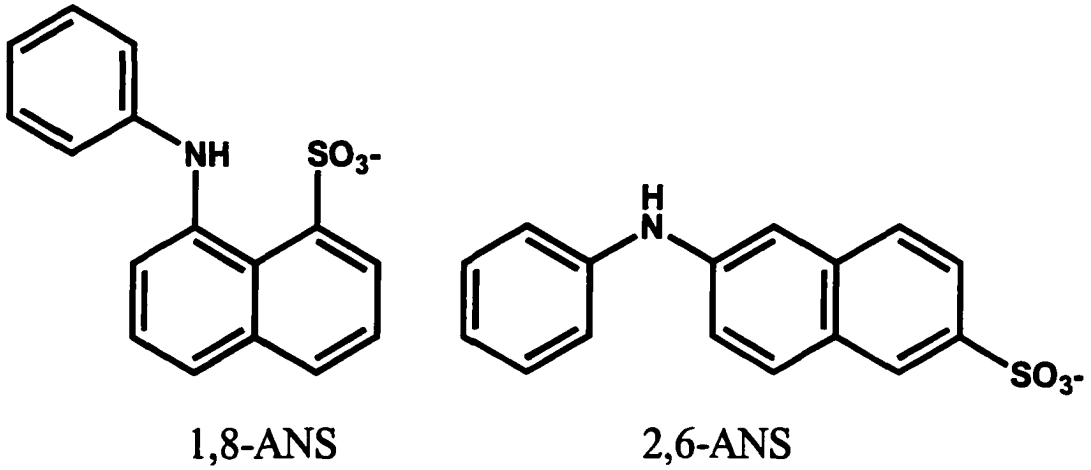

Figure 8. *Molecular Structures of 1,8-ANS and 2,6 ANS.*

These two probes are from the group of ANS isomers which have found extensive application due to their extremely high sensitivity to polarity. For example, they are nearly non-fluorescent in aqueous solution, but extremely fluorescent in a less polar solvent, such as ethanol. They have been extensively used in studies of host-guest inclusion complexes by cyclodextrins, by our group and others [39, 40]. These two probes differ only in the positions of the anilino and sulfonate groups on the naphthalene fluorophore. Isomer 1,8-ANS has the two groups substituted on the same long side of the naphthalene ring, which makes 1,8-ANS a much bulkier molecule than the 2,6-ANS isomer, which has the anilino and sulfonate groups located on opposite ends of the naphthalene fluorophore, making it narrower, longer,

and more streamlined. Wagner *et al.*[15,20,39] showed that as a result of this significant structural difference, the two ANS probes exhibit significant differences in formation of host-guest inclusion complexes with parent and substituted cyclodextrins as well as with the parent cucurbituril, CB[6]. Therefore, in this project for the first time, detailed investigations of the formation of the host-guest inclusion complexes between cucurbituril homologue CB[7] and the above mentioned fluorophores in solution as well as their association constants are described.

In addition to these two probes, various other fluorescent probes, as shown in Figure 9, were tried with water-soluble calix[n]arenes, including Dansyl Lysine, Nile Red, Nile Blue, Neutral Red, Resorufin and lanthanides.

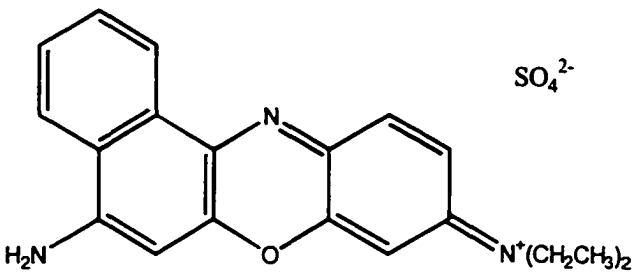

1

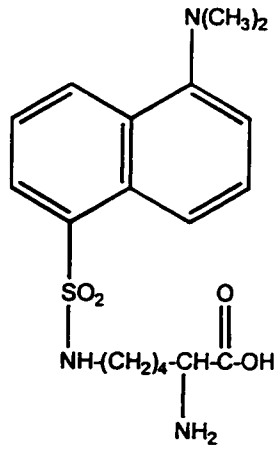

2

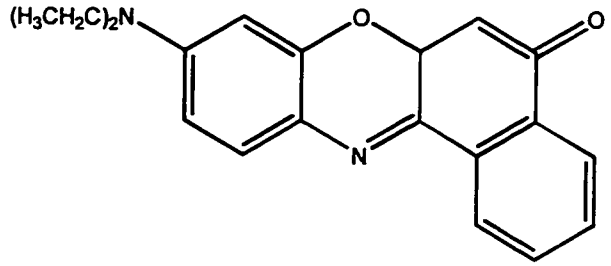

3

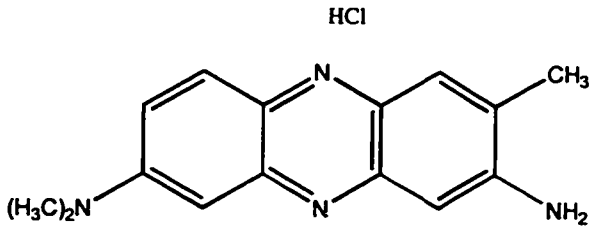

4

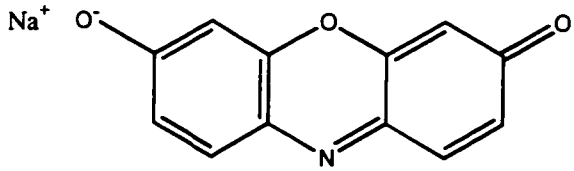

5

Figure 9. *Molecular structures of 1 Nile Blue, 2 Dansyl Lysine, 3 Nile Red, 4 Neutral Red, and 5 Resorufin.*

II. *EXPERIMENTAL*

II.1 *Chemical Sources*

The chemicals used for this project and their sources are listed in Table 1. All were used as received.

Chemicals	**Supplier (s)**
p-sulfonic calix[4]arene	Acros and Spectrum
p-sulfonic calix[6]arene	Acros and Spectrum
Cucurbit[7]uril	Received from Dr.Rodney Blanch, University of New South Wales, Australia
2,6-ANS	Molecular Probes
1,8-ANS	Aldrich Chemical Co.
Resorufin	Molecular Probes
Dansyl Lysine	Molecular Probes
Nile Red	Aldrich Chemical Co.
Nile Blue	Aldrich Chemical Co.
Neutral Red	Aldrich Chemical Co.
DMP	Aldrich Chemical Co.
$Eu(III)Cl_3$	Aldrich Chemical Co.
$Sm(III)Cl_3$	Aldrich Chemical Co.

Chemicals	Supplier
Methanol	Aldrich Chemical Co.
Ethanol	Aldrich Chemical Co.
n-butanol	Fisher Scientific Company
Isopropanol	Fisher Scientific Company
Acetonitrile	Fisher Scientific Company
Acetone	Fisher Scientific Company
Dichloromethane	Fisher Scientific Company
Ethylacetate	Fisher Scientific Company
Cyclohexene	Fisher Scientific Company

Table 1: *List of chemicals used for this project.*

II.2 *Sample Preparation*

In this project, different experimental methods were used for preparing the solutions, with respect to the two different host molecules used.

II.2.1 *Cucurbit[7]uril Sample Preparation*

During the course of this project, three different samples of CB[7] were received. The first sample of CB[7] was 80% pure with the major contaminant being CB[5], which is insoluble in aqueous solution, resulting in the poorest solubility of this CB[7] compared

with the other two. The last two samples received were 99 % pure by NMR, except that one of them contained water and HCl (corrections were not done for the content of water).

Stock solutions of the ANS molecules were made in KH_2PO_4/K_2HPO_4 buffer (pH=6.8) prepared from ultrapure distilled water (from D0836 MACRO Pure Cartridge), having concentrations of $2x10^{-5}$ M (1,8-ANS) and $9x10^{-5}$ M (2,6-ANS) as well as in 0.2M Na_2SO_4 solution with the same concentrations of 1,8-ANS and 2,6-ANS. At these concentrations the ANS molecules had an absorbance between 0.20 and 0.40 at the excitation wavelength of 370 nm. Solutions of ANS molecules with cucurbit[7]uril of various concentrations were prepared by adding the appropriate amount of solid cucurbit[7]uril to the ANS stock solutions. In addition, due to the fact that only small amount of cucurbit[7]uril solid could be obtained from the supplier (1.0 g), some of solutions of ANS molecules with cucurbit[7]uril of various concentrations were prepared by dilution. In order to obtain a measure of the relative polarity of cucurbit[7]uril cavity the emission maxima of both ANS molecules were determined in a number of pure and mixed solvents.

II.2.2 *p-Sulfonic Calix[n]arenes Sample Preparation*

Every stock solution of probe molecules used in the calixarene experiments was made in ultrapure distilled, de ionized water. Solution concentrations were adjusted to give an absorbance of 0.30 at the chosen excitation wavelength. Solutions of probe molecules with *p*-sulfonic calix[4]arene and *p*-sulfonic calix[6]arene of various concentrations were

prepared by adding the appropriate amount of solid to the probe stock solutions.

In the case when Nile Red (almost insoluble in water) was used as a guest molecule, two different experimental methods were used for preparing the solutions. In the first method (Method A), solutions of Nile Red and calixarene of interest were prepared by transferring Nile Red and calixarene solids to volumetric flasks to obtain desired concentration of calixarene and $1x10^{-4}$ M concentration of Nile Red. The flasks were then filled with nanopure de ionized water. These mixtures were then placed in an ultrasonic bath for at least ten minutes. After sonicating, solutions were allowed to sit at room temperature overnight in dark. The undissolved Nile Red solid was removed by filtration and then both absorbance and fluorescence spectra of filtered solutions were collected.

In the second method (Method B), solutions of Nile Red and calixarene of interest were prepared as follows: an excess amount of Nile Red was added to nanopure water initially. Since Nile Red is almost insoluble in water, this solution was stirred for several hours and then allowed to sit at room temperature in the dark for 24 hour in order to obtain a saturated Nile Red solution. On the next day, undissolved Nile Red solid was removed by filtration. Solutions of Nile Red and calixarene of interest were prepared by dissolving appropriate amount of solid calixarene to the Nile Red stock solution. Both absorbance and fluorescence spectra were then collected.

Crystals of *p*-sulfonic calix[4]arene and $Eu(III)Cl_3$ complex were prepared by mixing of 0.1M solution of $Eu(III)Cl_3$ with 50mM solution of *p*-sulfonic calix[4]arene, both in nanopure water. The crystals were suction filtered and air dried, yielding fine white powder. Also crystals of the same complex were prepared by diffusion method, where

solution of above mentioned concentrations were allowed to mix slowly by diffusion in two connected test tubes.

In the course of this project, two different types of calixarene samples were purchased. The initial samples of *p*-sulfonic calix[4]arene and *p*-sulfonic calix[6]arene were of high quality, and were white solids with low absorbance. Unfortunately, all subsequently purchased samples from both sources listed in Table 1 were impure, grey coloured solids, showing high absorbance. This severely hindered our spectroscopic studies of the inclusion complexes of these calixarenes. An attempt at purification of this grey powder was performed by repeating the last few steps of the calixarene synthesis done by Shinkai and co-workers *et al.*[29]. 0.47 g of either *p*-sulfonic calix[4]arene or *p*-sulfonic calix[6]arene, used as received, was dissolved in 10 mL of hot nanopure water. After the mixture was cooled, Na_2SO_4 was added until pH = 8 was obtained. The solution was then filtered under vacuum, and approximately 80-100 mL of methanol was slowly added to the filtrate. After the addition of methanol the mixture was placed in a refrigerator for 24 hours; a precipitate was formed, which was collected and dried. However, the purified calixarene sample still showed very high absorbance throughout the spectroscopic region of interest.

II.3 *Absorption Studies*

If significant changes occur in the absorption spectrum of the guest molecule upon complexation within the host, then absorption spectroscopy can also be used as a tool to provide useful information about the complex stability constant as well as complex

stoichiometry. Moreover, the nature of the spectral changes provides information on the number of complexes present. For example, one or two isosbestic points observed in the absorbance spectrum over the full range of the host concentrations can indicate that only a single complex stoichiometry is present. However, loss of the isosbestic behaviour as a function of changing the host concentration would mean that at least two complexes of different stoichiometry are present. In the case when calixarenes were used as host molecules, significant changes in absorbance spectra of guest molecules were observed.

All absorption spectra were measured using a Cary 50 Bio UV- Visible Spectrophotometer. The changes observed in the absorbance (ΔA) as a function of the calixarene concentration are related to the association equilibrium constant K according to equation:

$$\Delta A = K \Delta\varepsilon \, [\text{calixarene}] / (1 + K[\text{calixarene}]) \quad (12)$$

where $\Delta\varepsilon$ is the difference between the molar extinction coefficients for complexed and free guest. The numerical values for the binding constants were determined using a non-linear least-squares analysis program.

II.4 *Steady-State Fluorescence*

Steady-state fluorescence spectra were performed using two Photon Technologies International LS-100 fluorimeters (PTI #1 and PTI #2, which differ mainly in age), with

excitation and emission monochrometer bandpasses adjusted to optimize the fluorescence signal in each set of experiments, and the excitation wavelength set at a specific wavelength, depending upon the probe molecule of interest used. Sample solutions of interest were transferred to a 1.0 cm^2 quartz cuvette, and placed into the sample holder of the fluorimeter. The light passes through excitation monochromator (set at fixed wavelength) hitting the sample which partially absorbs the light. This absorption of light causes the excitation of the sample and emits the fluorescence in all directions, but only emission discharged at 90° will be detected. The emission light then passes through the emission monochromator onto the detector (photomultiplier tube). The detector signal is collected by a computer which also controls the scanning of the excitation and emission monochromators. By fixing the excitation monochromator at the desired wavelength and scanning the emission monochromator, an emission spectrum of fluorescence intensity versus emission wavelength (I_F *vs.* λ) is obtained. Therefore, fluorescence intensity is measured as the number of photons that hit photomultiplier tube per second, or counts per second (cps). The excitation and emission wavelengths were chosen regarding the particular host and guest molecules used in the experiment. The data were collected, recorded and analysed by the software for the PTI instrument (Felix Fluorescence Analysis Software). The analysed data plots were made with Fig.P, version 2.7, plotting software.

The fluorescence enhancement, F/F_0, was determined as the ratio of the integrated area under fluorescence spectrum (I_F *vs.* λ) of guest molecule in the presence and absence of the host of interest, where F is the total fluorescence in the presence of the host, and F_0 is the total fluorescence in the absence of the host:

$$F/F_0 = \int I_F \, d\nu \, / \int I_{F0} \, d\nu \qquad (13)$$

II.5 *Determination of Association Constants (K)*

For a 1:1 host-guest complex, the binding equilibrium constant K can be defined as follows:

$$\text{Host} + \text{Guest} \rightleftarrows \text{Host:Guest} \qquad (14)$$

$$K = [\text{Host:Guest}] \, / \, [\text{Host}] \, [\text{Guest}] \qquad (15)$$

The numerical value of K can be obtained from the observed fluorescence enhancement (F/F_0) as a function of added host concentration ($[host]_0$) using the following equation[40]:

$$F/F_0 = 1 + (F_\infty/F_0 - 1) \, [host]_0 K \, / \, (1+[host]_0 K) \qquad (16)$$

where F is the integrated fluorescence intensity in the presence of the host, F_0 is the integrated fluorescence intensity in the absence of the host, and F_∞ is the integrated fluorescence intensity when all guest molecules have been complexed by host molecules.[40]

For 2:1 host-guest complexation the binding equilibrium constants K_1 and K_2 can be defined as:

$$\text{Host} + \text{Guest} \rightleftarrows \text{Host:Guest} \tag{17}$$

$$K_1 = [\text{Host:Guest}] / [\text{Host}]\,[\text{Guest}] \tag{18}$$

$$\text{Host:Guest} + \text{Host} \rightleftarrows (\text{Host})_2\text{:Guest} \tag{19}$$

$$K_2 = [(\text{Host})_2\text{:Guest}] / [\text{Host:Guest}]\,[\text{Host}] \tag{20}$$

The numerical values of K_1 and K_2 binding constants can be determined using the following equation:

$$F/F_0 = (1 + F_a K_1[\text{host}] + F_b K_1 K_2[\text{host}]^2) / (1 + K_1[\text{host}] + K_1 K_2[\text{host}]^2) \tag{21}$$

where $F_a = F_1/F_0$, $F_b = F_2/F_0$, F is the integrated fluorescence intensity in the presence of the host, and F_0 is the integrated fluorescence intensity in the absence of the host molecules.

The numerical values for the binding constants were determined using non-linear least-squares analysis programs, written by Dr. B. D. Wagner, based on equations 16 and 21. In all cases, a total of 10-15 individual data pairs of (F/F_0, [host]) were analysed to obtain the value of K. Furthermore, at least three separate trials were performed, and the calculated K values were averaged for each host-guest pair. The fit parameters were then used to plot the fitted curves of F/F_0 *vs.* [host], and compared with experimental data.

II.6 *Temperature Studies*

The temperature in the fluorimeter was controlled using a Fischer Scientific Isotemp 1016 temperature control bath. The temperature range was from 9-49 °C, in five 10 °C increments for CB[7] + 2,6-ANS in potassium phosphate buffer. In all cases, at least two trials for each set of data were collected at the above mentioned temperatures. The concentrations of CB[7] ranged from 0.25mM to 10mM. The spectrum of each CB[7]:2,6-ANS system was collected, both in the absence and presence of CB[7] molecules. For each set of spectra, the fluorescence enhancement factors, F/F_0, were then calculated at the various concentrations of host molecule, CB[7]. The association constants, K, were determined using the computer program to fit fluorescence enhancement vs. cucurbituril concentration data to the 1:1 host:guest complex (equation 16), using non-linear regression techniques. The values for these constants were then averaged between the appropriate trials for given temperatures. The natural log of the association constant, ln K, was plotted against 1/T, where T is the temperature in Kelvin, using the Fig. P program. In addition, this plot was used to obtain the thermodynamic quantities of interest.

II.7 *Time Resolved Fluorescence*

The three most common types of fluorescence lifetime measurements performed are phase modulation, the stroboscopic (strobe) method, and single photon counting.[6] The last two methods have an advantage over the phase modulation method in that they allow the

fluorescence decay curve to be measured directly. The stroboscopic (strobe) method, which was employed in this project, was initially developed by Bennet, and later improved by James *et al.*[12] The strobe technique has several advantages. It is intensity based which means that intensity of the signal is directly proportional to the intensity of the lamp.[12] Therefore, the instrument can measure signal with each flash of the lamp, thus providing a faster rate of data acquisition than the time-correlated single photon counting technique which can use one flash in twenty.[40] Therefore, with a more intense lamp, data can be acquired more quickly and with a better signal-to-noise ratio.[12] The instrumentation used in this technique is less expensive and complex than in other methods, as well as it is computer controlled which thus greatly simplifies its use and operation.

In this project, the fluorescence decay measurements were performed with the Photon Technology International Time Master Fluorescence Lifetime Spectrophotometer. A potassium phosphate buffer solution of known dye concentration ($9x10^{-5}$ M 2,6-ANS) was used to dissolve weighed amounts of CB[7] in order to obtain the desired concentrations (0,2,4, 6, 8 and 10mM). All of these buffer solutions were both argon purged and non-purged in order to determine whether there was any oxygen effect on the fluorescence lifetime of the 2,6 ANS molecules (none was found). The fluorescence lifetime of 2,6-ANS in ethanol was measured as well, as it had been shown that the polarity of the CB[7] cavity is close to that of ethanol. An excitation wavelength of 370 nm was used, and the decays were analysed by one, two and three exponential fit analysis using the software available with the instrument. The software can fit up to four exponential decays, and uses the fitting law:

$$I_F(t) = \sum a_i e^{-t/\tau} \quad (22)$$

where a_i is the preexponential factor, and $I_F(t)$ is the fluorescence decay curve. The preexponential factor assigned to a lifetime is a mathematical weighting factor for that lifetime value in the overall fluorescence decay. The χ^2 value is an indication of how good the exponential fit is to the actual decay. The closer its value is to unity, the better is the fit to the actual fluorescence decay. If only one type of complex is formed between 2,6-ANS and CB[7] molecules, the solution will have a single exponential decay, giving one value for the fluorescence lifetime. If upon complexation with CB[7], 2,6-ANS molecules experience several distinct environments, or form several types of complexes with CB[7] or they are even complexed to different degrees by the host, then multiple exponential decay constants will be obtained as well as a fluorescence lifetime for each of the different emitting species.

III. *INCLUSION COMPLEXES OF CUCURBIT[7]URIL*

III.1 *Fluorescence Enhancement Studies*

As mentioned previously in the experimental section, three different samples of CB[7] were received during the course of this project. The first sample of CB[7] was 80% pure with the major contaminant being CB[5], which is insoluble in aqueous solution, resulting in the poorest solubility of this CB[7] compared with the other two. The last two samples received were 99 % pure by NMR, except that one of them contained water and HCl. Due to the difference in purity of the CB[7] samples, slight differences in results of fluorescence intensity as well as binding constant were obtained among different trials. In addition, two different aqueous solutions were used, potassium phosphate buffer and 0.2 M Na_2SO_4, since CB[7] is not soluble in pure water. Initially, experiments were done in 0.2 M Na_2SO_4, however since the ANS molecules are acids, it was decided to perform experiments in potassium phosphate buffer solution as well in order to maintain the pH of the solution.

III.1.1 *2,6-ANS Results in Potassium Phosphate Buffer and 0.2M Na_2SO_4*

The fluorescence spectrum of 2,6-ANS in potassium phosphate buffer (pH=6.8) was found to increase significantly in intensity upon addition of CB[7], by a maximum factor of 25 at high CB[7] concentration, as shown in Figure 10. This increase in fluorescence

intensity indicates the formation of a host-guest inclusion complex of 2,6-ANS within the CB[7] cavity. However, as can be seen from Figure 10, there was very little shifting of the spectrum, with a fluorescence maximum of 459 ± 2 nm in the absence of CB[7] and 452 ± 2 nm in the presence of 10 mM CB[7].

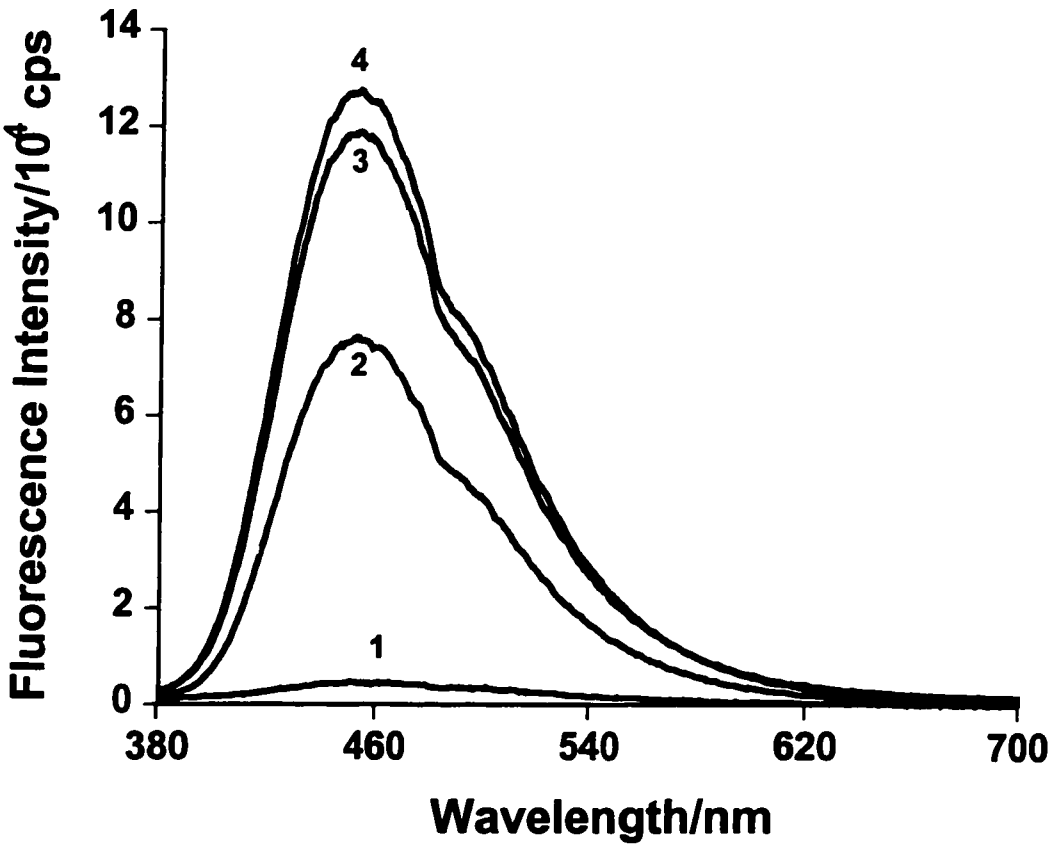

Figure 10. *Fluorescence spectra of 2,6-ANS in the presence of various amounts of CB[7]*: 1 *0 mM;* 2 *2 mM*; 3 6 mM; 4 *10 mM.*

The fluorescence enhancement was measured as a function of [CB[7]] from 0 to 10 mM in potassium phosphate buffer (99% pure CB[7] was used). After determination of numerical values for the binding constant for 1:1 host-guest complex, and calculation of the fitted values for the fluorescence enhancements by fitting the F_∞/F_0 and K as fit parameters into Equation 16, it was determined that 2,6-ANS and CB[7] form a 1:1 host-guest inclusion complex. This also was confirmed by the double reciprocal plot (known as a Benesi-Hilderbrand-type plot) of $1/(F/F_0 - 1)$ vs. 1/[CB[7]]; this plot will be non-linear if higher-order complexes are formed. The enhancement data are shown in Figure 11, where the data points are the average values from three trials. The line of best fit, shown as the solid line in Figure 11, yielded a value of $K = 490 \pm 80\ M^{-1}$, with $F_\infty/F_0 = 25 \pm 3$. The corresponding reciprocal plot, shown in Figure 12, is linear ($R = 0.9995$) confirming simple 1:1 host-guest complexation.

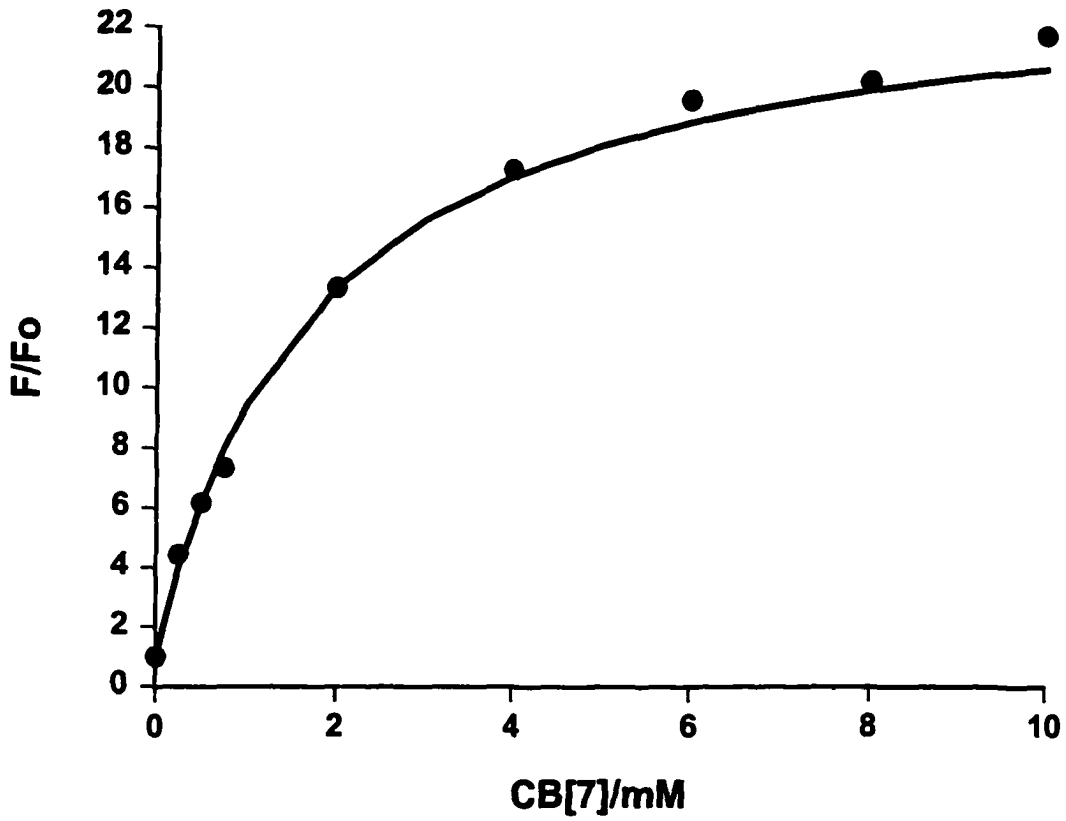

Figure 11. *The fluorescence enhancement of, F/F_0, of 2,6-ANS in potassium phosphate buffer as a function of CB[7] concentration.*

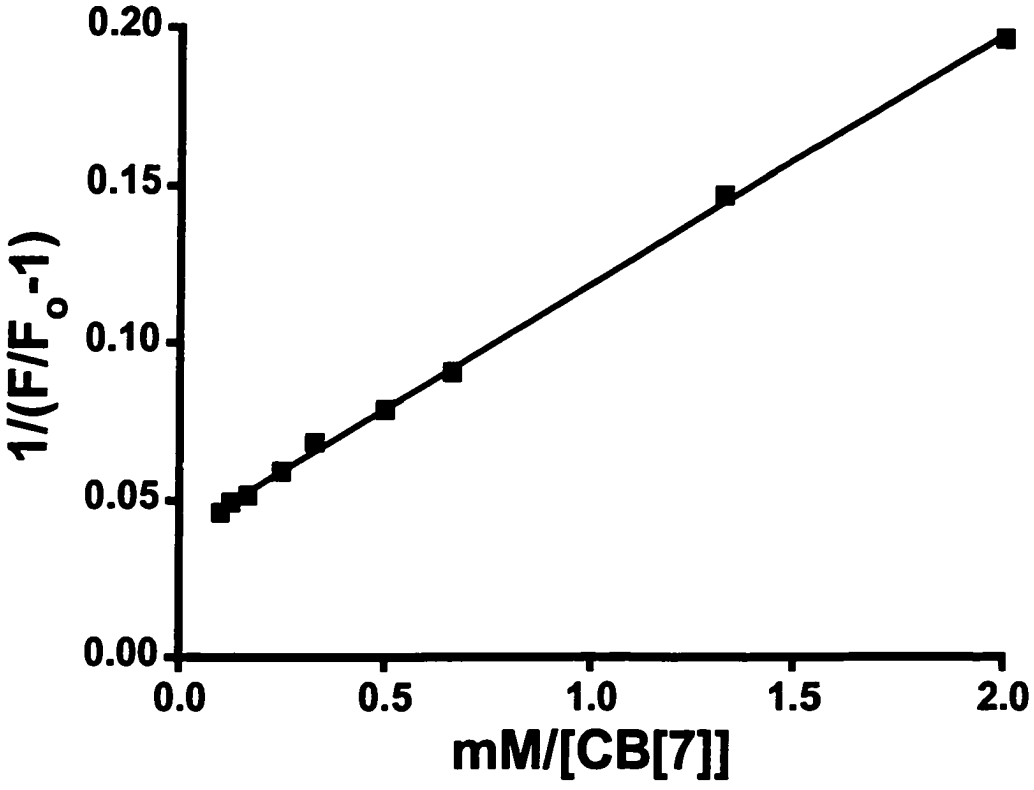

Figure 12. *Reciprocal plot of $1/(F_o/F - 1)$ vs. 1/[CB[7]] for 2,6-ANS.*

In the case when aqueous 0.2 M Na_2SO_4 solution was used as medium, the fluorescence enhancement was measured as a function of [CB[7]] (80% pure CB[7] was used) from 0 to 6 mM. Similar results were obtained compared with those in buffer, with an increase in fluorescence intensity by a factor of 25 as well. Also, it was determined and confirmed by double reciprocal plot of $1/(F/F_0 - 1)$ vs. 1/[CB[7]], which was linear, that 1:1 host:guest complex is formed, with the binding constant of $K = 244 \pm 98\ M^{-1}$ (averaged over three trials). There was also very little shifting of the spectrum, with a fluorescence maximum of 458 ± 2 nm in the absence of CB[7] and 446 ± 2 nm in the presence of 6 mM CB[7].

III.1.2 *1,8-ANS Results in Potassium Phosphate Buffer and 0.2M Na_2SO_4*

The fluorescence of 1,8-ANS was also found to increase significantly in intensity upon the addition of CB[7] to the both potassium phosphate buffer and 0.2M Na_2SO_4 solutions, as shown in Figure 13, indicating the formation of a host-guest inclusion complex of 1,8-ANS within the CB[7] cavity.

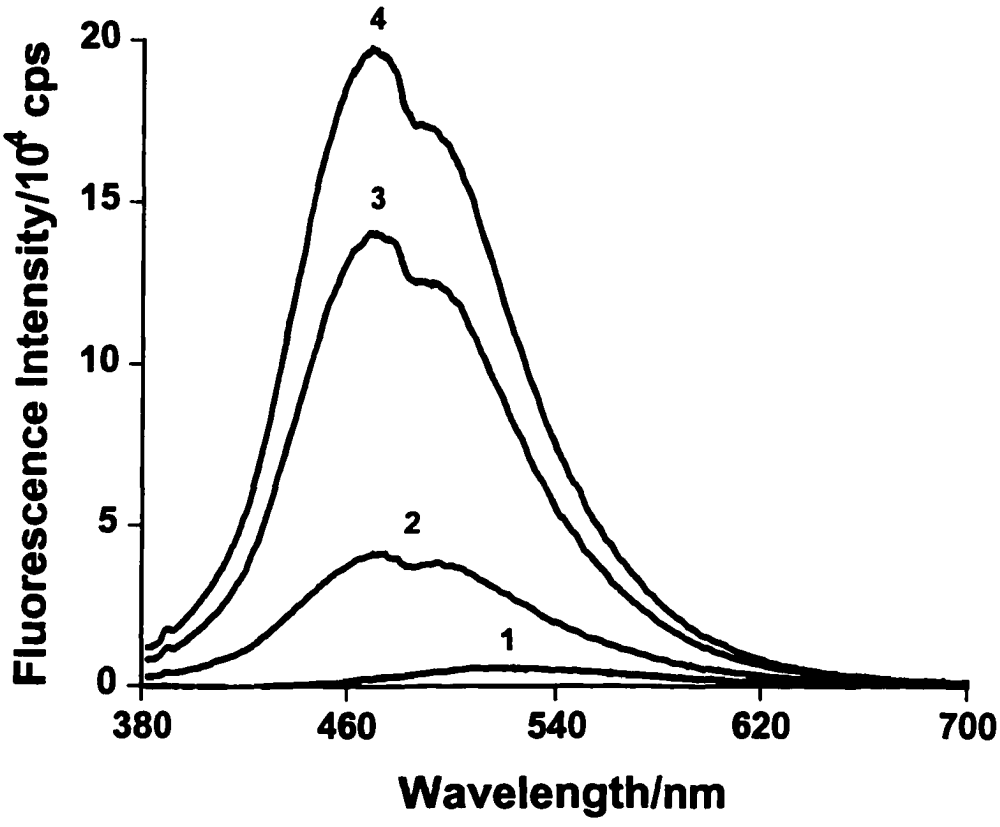

Figure 13. *Fluorescence spectra of 1,8-ANS in the presence of various amounts of CB[7] in potassium phosphate buffer* :**1** *0 mM;* **2** *2 mM*; **3** 6 mM; **4** *10 mM.*

Contrary to the case of 2,6-ANS, there was significant blue shifting of the spectrum, with a fluorescence maximum of 517 ± 2 nm in the absence of CB[7] and 469 ± 2 nm in the presence of 15mM CB[7]. Figure 14 shows the plot of fluorescence enhancement as a function of CB[7] concentration (averaged over three trials in buffer solution). This plot has a very different shape than that seen in Figure 10 for 2,6-ANS, suggesting the formation of higher order complexes. This was confirmed by the double reciprocal plot shown in Figure 15, which is clearly nonlinear.

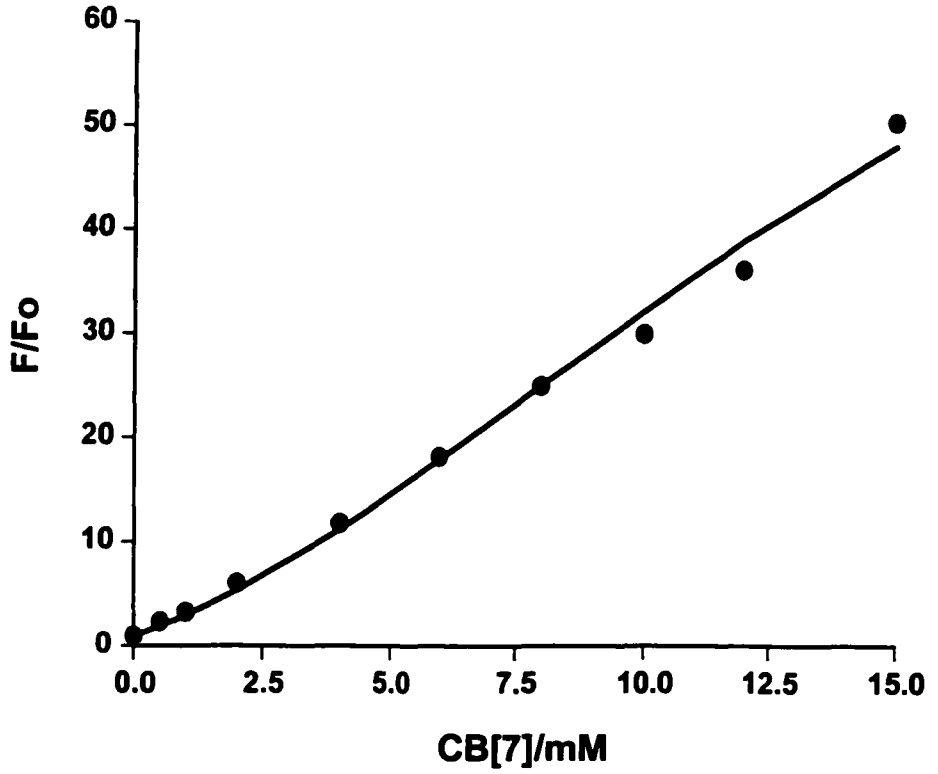

Figure 14. *The fluorescence enhancement of, F/F_0, of 1,8-ANS in potassium phosphate buffer as a function of CB[7] concentration.*

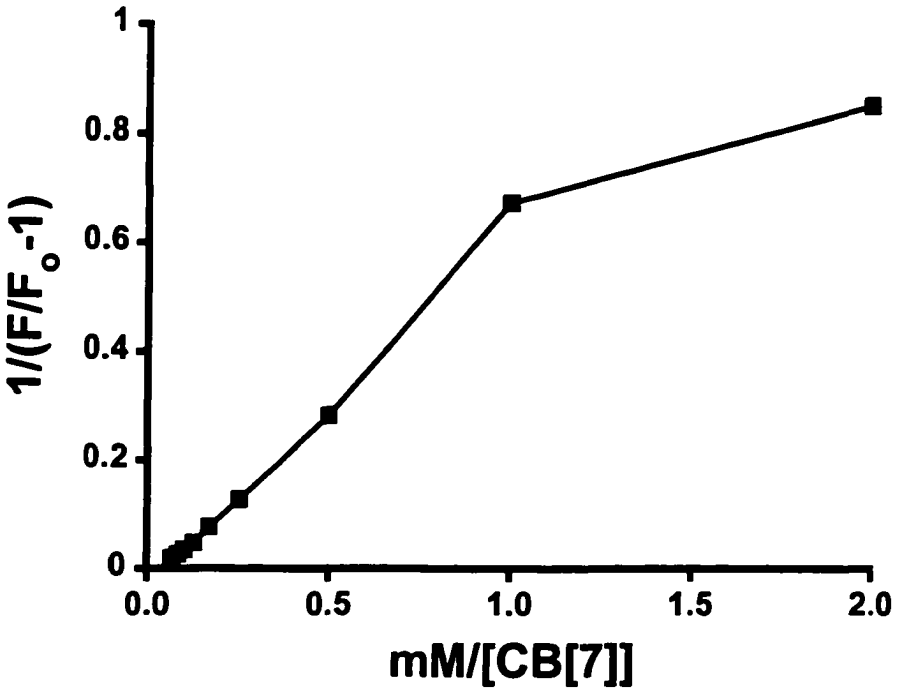

Figure 15. *Reciprocal plot of F_0/F -1 vs. 1/[CB[7]] for 1,8-ANS.*

The fluorescence enhancement was measured as a function of [CB[7]] from 0 to 15 mM in potassium phosphate buffer (99% pure CB[7] was used]. After determination of numerical values for binding constants for 1:1 and 2:1 host-guest complexes, and calculation of the fit values for the fluorescence enhancements by fitting the F_1/F_0 and F_2/F_0 (the fluorescence intensities of the 1:1 and 2:1 complexes, respectively), K_1 (equilibrium constant for formation of the 1:1 complex), and K_2 (the equilibrium constant for the formation of 2:1 complex from addition of a second host to the 1:1complex), as fit parameters into

Equation 21, it was determined that 1,8-ANS and CB[7] form 2:1 host-guest inclusion complexes. The solid line in Figure 14 shows the excellent fit of the data to Equation 21, yielding the values $F_1/F_0 = 84 \pm 24$, $F_2/F_0 = 158 \pm 14$, $K_1 = 11 \pm 3\ M^{-1}$ and $K_2 = 190 \pm 22\ M^{-1}$. By contrast, a much poorer fit was obtained using Equation 16 for 1:1 complexation, as well as using the equations derived in the literature[42] for 1:2 and 2:2 complexation.

In the case when the aqueous 0.2 M Na_2SO_4 solution was used as solvent, the fluorescence enhancement was measured as a function of [CB[7]] (80% pure CB[7] was used) from 0 to 10mM. Similar results were obtained compared with those in buffer, yielding the values of $F_1/F_0 = 21$, $F_2/F_0 = 90$ $K_1 = 44\ M^{-1}$ and $K_2 = 382\ M^{-1}$ (averaged over three trials). Also, it was determined and confirmed by the double reciprocal plot of $1/(F/F_0 - 1)$ vs. 1/[CB[7]], which was nonlinear, that higher-order, 2:1 CB[7]:1,8-ANS, complexes are formed. There was also significant blue shifting of the spectrum, with a fluorescence maximum of 518 ± 2 nm in the absence of CB[7] and 471 ± 2 nm in the presence of 10mM CB[7].

III.1.3 *Discussion*

The significant enhancement of the fluorescence of 2,6-ANS by CB[7], by a factor of 25, was observed in both potassium phosphate buffer and 0.2 M Na_2SO_4 solutions. The excellent fit of the enhancement as a function of CB[7] concentration data in both solvents to Equation 16, and the linear double reciprocal plot, indicate that simple 1:1 complexation is occurring between the 2,6-ANS guest and CB[7] host, with binding constants of $490 \pm$

80 M^{-1} and 244 ± 98 M^{-1} , in potassium phosphate buffer and 0.2 M Na_2SO_4, respectively. The difference in the binding constants of the CB[7]:2,6-ANS complexation in two different solvents can be explained by the fact that all measurements in potassium phosphate buffer were done using the 99% pure CB[7] as a host, while measurements in 0.2 M Na_2SO_4 solution were performed using the 80% pure CB[7], where the major contaminant was insoluble CB[5]. The difference in the purity of the CB[7] samples is the main reason why the highest possible concentration of CB[7] used in 0.2 M Na_2SO_4 solution is 6 mM, while in potassium phosphate buffer solution is 15 mM. The lack of a significant blue-shift in the spectrum, in both solvents, suggests that only the phenyl moiety is inserted into the CB[7] cavity, rather than the naphthalene moiety. If the naphthalene moiety is being included, then a much larger blue shift of the 2,6-ANS spectrum would be expected. For example, inclusion of 2,6-ANS into modified β-cyclodextrins, which involves naphthalene inclusion, results in 28-40 nm blue shift in the 2,6-ANS spectrum.[40] Also, in the complexation studies of 2,6-ANS and CB[6] by Wagner *et. al.*[20], it was determined that a 1:1 complex is formed with no significant blue shift in the 2,6-ANS spectrum, suggesting again that only the phenyl moiety is included within the host cavity. In the case of naphthalene inclusion (such as in modified cyclodextrins), the observed fluorescence enhancement is a result of the reduced local polarity experienced by the naphthalene fluorophore within the host cavity as compared with the aqueous solution. In the case of phenyl inclusion, a different mechanism for fluorescence enhancement is required. Inclusion of the phenyl part of the probe molecule into the CB[7] cavity results in a significant reduction of the intramolecular rotation freedom of phenyl ring relative to the naphthalene ring.[43,44] This results in a decrease in the rate of

intramolecular charge transfer, which requires an intramolecular twisting of the phenyl ring relative to the naphthalene fluorophore. This charge transfer followed by energy transfer, represents a significant non-radiative decay pathway for anilinonaphthalenes in polar environments.[20] The reduction of the rate for this process reduces the overall rate for non-radiative decay of the 2,6-ANS excited state, resulting in an increase in the fluorescence quantum yield, and therefore the measured fluorescence enhancement.

The results presented here represented not only the first reported association constant for an inclusion complex of CB[7], but also allow for the direct comparison of the host properties of CB[7] with that of the original cucurbituril, CB[6], since 2,6-ANS as a guest has now been studied in both related hosts.

As previously reported by Wagner *et. al.*[20], the maximum fluorescence enhancement of 2,6-ANS fluorescence in CB[6] by factor 5 was observed, which is significantly lower than the maximum fluorescence enhancement of 25 observed here for 2,6-ANS in CB[7]. This indicates that inclusion of the phenyl group into the larger CB[7] results in a much greater reduction in the rate of the charge transfer decay process. Furthermore, the association constant of $490 \pm 80\ M^{-1}$ for 2,6-ANS with CB[7] is significantly larger than that of $52 \pm 10\ M^{-1}$ reported for 2,6-ANS in CB[6]. This suggests that a much stronger complex is formed between 2,6-ANS and CB[7] as compared with CB[6]. Thus, the larger cavity and portal (7.3 Å and 5.4 Å, respectively) of CB[7], makes it a much better size match and host for the 2,6-ANS phenyl ring than CB[6] with the cavity and portal of 5.8 Å and 3.9 Å, respectively, resulting in a much larger fluorescence enhancement as well as in a much stronger inclusion complex. Thus, CB[7] is seen to have significantly improved host

properties over the original cucurbituril, as a result of its more spacious internal cavity.

The results obtained by studying the complexation of 1,8-ANS with CB[7] are very different than those of 2,6-ANS. The maximum fluorescence enhancement of 120 is much larger than that of 25 observed for 2,6-ANS. Also, significant blue shifting of the 1,8-ANS spectrum by 48 nm is observed, while for 2,6-ANS the observed blue shift is only 7 nm. Furthermore, the enhancement *versus* CB[7] concentration data and double reciprocal plot clearly indicate the formation of the higher-order inclusion complexes than the simple 1:1 complexes indicated for 2,6-ANS. The excellent fit of the data to Equation 21, and the lack of satisfactory fit to the equation for a simple 1:1 inclusion complex, suggests the formation of 2:1 CB[7]:1,8-ANS complexes as result of addition of the second CB[7] to the already formed 1:1 CB[7]:1,8-ANS complex.

It is difficult to determine which part of the guest molecule, the phenyl or naphthalene moiety, is complexed first. However, the initial 1:1 complexation could occur at either the phenyl or naphthyl group, followed by 2:1 complexation on the previously uncomplexed group. The results for the fluorescence enhancements determined from the fit to the Equation 21, suggests that the naphthalene moiety is included first, since the initial fluorescence enhancement is 84 upon 1:1 complexation, followed by a smaller increase to 158 upon 2:1 complexation. If the phenyl group was complexed first, that would result in a much higher increase in fluorescence enhancement upon 2:1 complexation. This is also supported by the relative size of the equilibrium constants for the two steps, with the K_1 value of 11 M^{-1} being significantly smaller than the K_2 value of 190 M^{-1}. There is a much better size match between the phenyl group and CB[7] cavity size than for the naphthalene

group. The value of 190 M^{-1} is also in reasonable agreement with the value of 490 M^{-1} obtained for inclusion of the phenyl moiety of 2,6-ANS. The lower value of the inclusion constant for the phenyl group of 1,8-ANS as compared with 2,6-ANS can be explained by the stearic effect of the adjacent sulfonate group in 1,8-ANS, which is on the other side of the molecule in 2,6-ANS, and thus has no effect. The fact that the large blue shift in the 1,8-ANS spectrum was observed at a very low CB[7] concentrations supports the hypothesis that the naphthalene fluorophore is included first.

The assignment of the strongly blue-shifted spectrum with a maximum at 469 nm to a complex in which the naphthalene moiety of 1,8-ANS is included in the host cavity is consistent with the results reported by Wagner and MacDonald [40] for inclusion of 1,8-ANS in modified cyclodextrins (where the naphthalene part of molecule is included into the cavity), in which the observed 1,8-ANS fluorescence maxima were in the range of 465-471 nm.

The major differences in complexation of 2,6-ANS and 1,8-ANS in CB[7] can be explained by a consideration of the differing geometries of the two ANS isomers, as shown in Figure 8 on page 27. These two probes differ only in the positions of the anilino and sulfonate groups on the naphthalene fluorophore. Isomer 1,8-ANS has the two groups substituted on the same side of the long naphthalene ring axes (Figure 16), which makes 1,8-ANS a much bulkier molecule than 2,6-ANS isomer, which has anilino and sulfonate groups located on the opposite long ends of the naphthalene fluorophore. 2,6-ANS is thus narrower and longer, and more streamlined. In general, naphthalene and its derivatives can be included into the cavity of supramolecular host in two different ways, as shown in Figure

16: axial inclusion, in which the naphthalene ring enters the cavity *via* its shorter dimension, and equatorial inclusion, in which the naphthalene ring enters the cavity via its longer dimension. Since 2,6-ANS molecule has anilino and sulfonate groups located on the opposite sides of the naphthalene fluorophore, they effectively prevent both axial and equatorial inclusion of the naphthalene ring. However, in the case of 1,8-ANS, equatorial inclusion is favoured over axial, due to the positions of the substituents. Thus, the geometric differences in these two isomers result in completely different complexation by CB[7] described above. Such significant differences in complexation of these two ANS isomers was also observed in their complexation with CB[6] as the host molecule. [20,45] In the case of 2,6-ANS, a 1:1 host-guest complex was observed in solution,[20] whereas in the case of 1,8-ANS, a solid precipitate was formed, which was found to be a lattice inclusion compound, in which the guest is excluded from the host cavity[45].

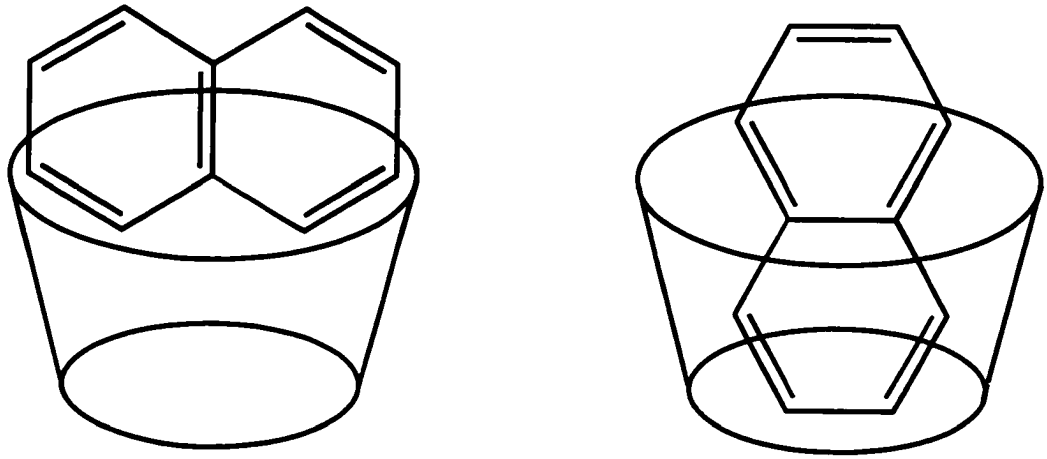

a) equatorial b) axial

Figure 16. *Axial and equatorial inclusion of 2,6-ANS molecule within the host cavity.*

III.2 *Cavity Polarity of CB[7]*

It is interesting to compare the spectra of the two probes included in CB[7] and in solvents of various polarities. Figures 17 and 18 compare the positions of the normalized spectra of 2,6-ANS and 1,8-ANS in aqueous buffer, methanol, and ethanol solutions, as well as in aqueous buffer in the presence of CB[7], respectively. The spectrum of 2,6-ANS in CB[7] is very similar to that in aqueous buffer, with only a small shift. On the other hand, the spectrum of 1,8-ANS in CB[7] is very similar to that of ethanol, with a significant shift. This fact clearly illustrates the difference in complexation of these two probes with CB[7], and clearly suggests the involvement of the naphthalene group in the case of 1,8-ANS, and its lack of involvement in the case of 2,6-ANS.

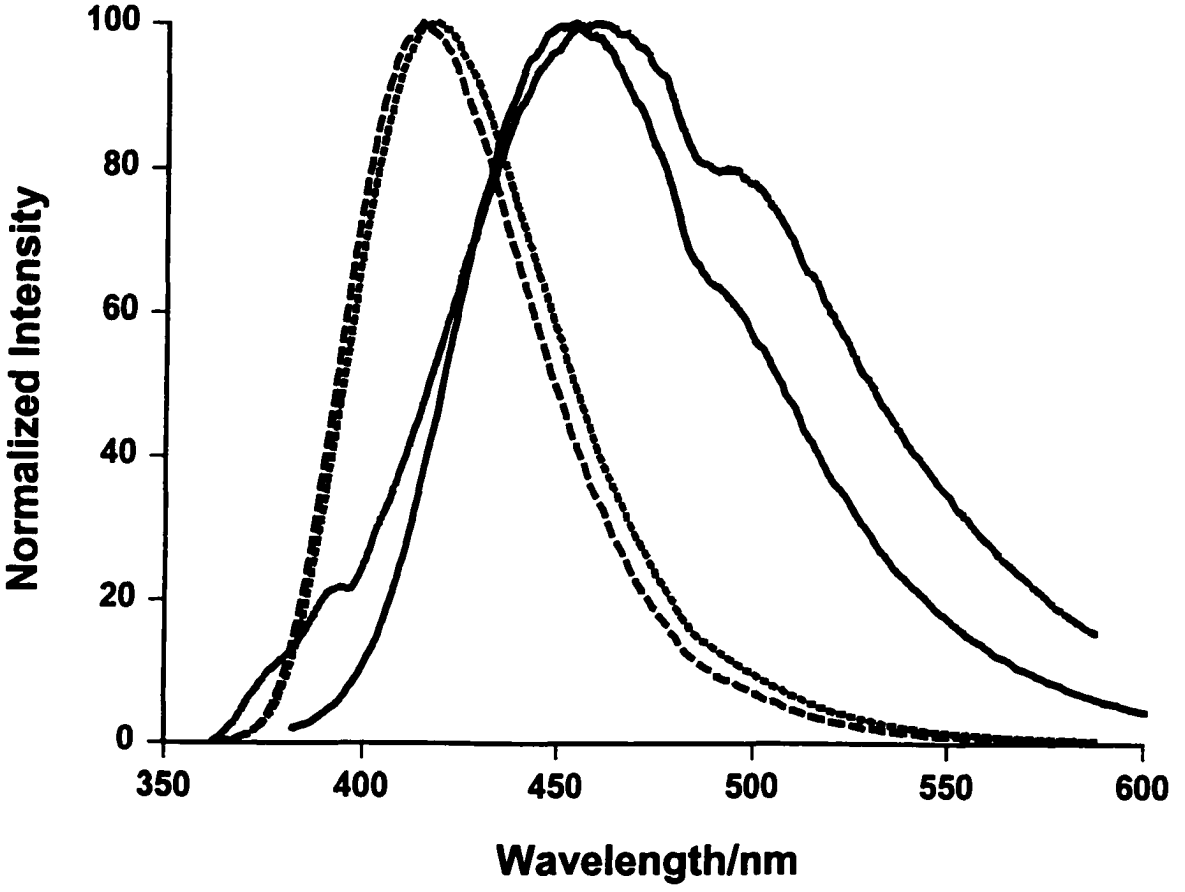

Figure 17. *Normalized fluorescence spectra of 2,6-ANS in H_2O buffer (__ .), methanol (...), ethanol (----), and in 10 mM CB[7] (___).*

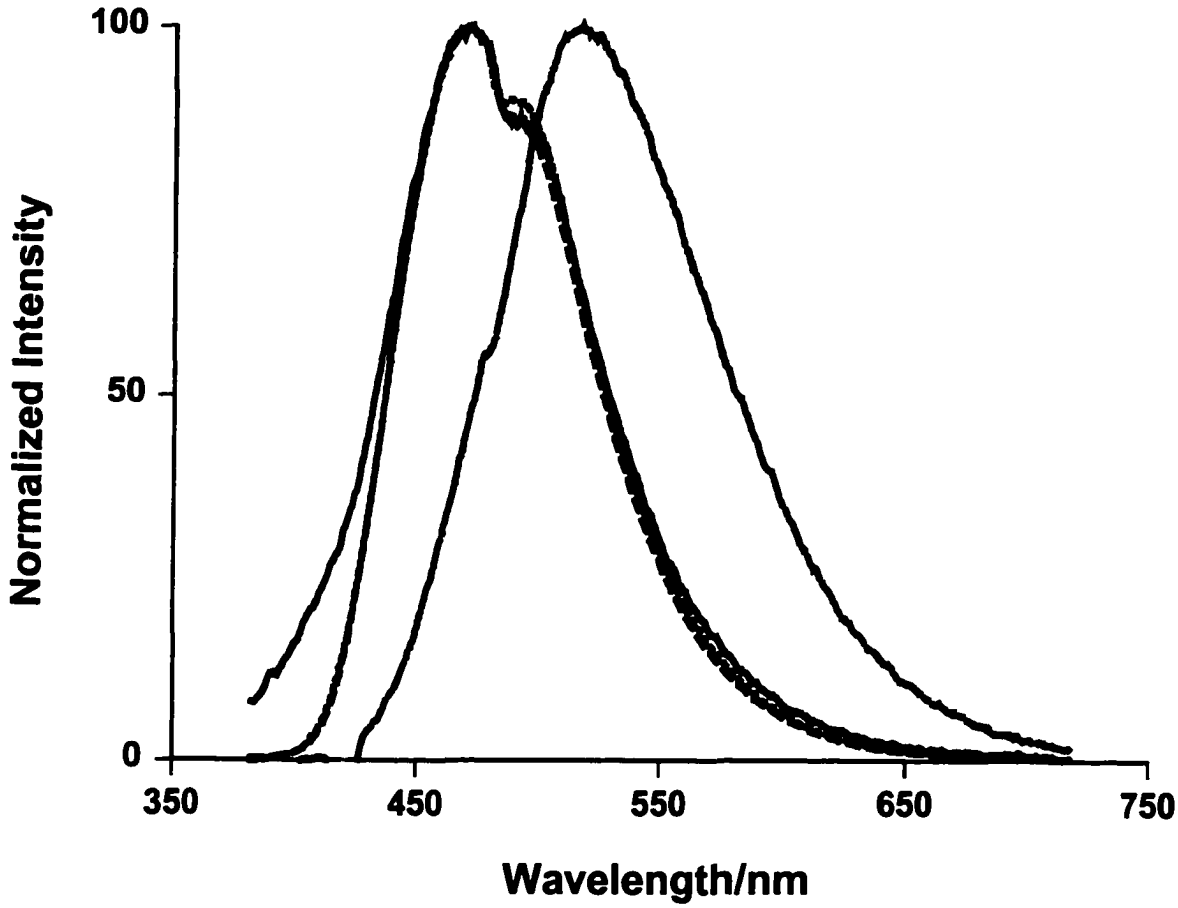

Figure 18. *Normalized fluorescence spectra of 1,8-ANS in H_2O buffer (__.), methanol (...), ethanol (----), and in 10 mM CB[7] (___).*

As can be seen from both Figures 17 and 18, and Table 2, there is a significant change in the shape of the fluorescence spectra of both 1,8-ANS and 2,6-ANS with a change in relative polarity of the solvents. For example, it is obvious that only one fluorescence maximum is observed for 1,8-ANS in aqueous buffer (519 nm). As the polarity of the solvent decreases, two emission maxima are observed (for example at 470.5 nm and 493.6 nm in ethanol). The opposite behaviour is observed in the case of 2,6-ANS with decreasing solvent polarity, where, for example, two fluorescence emission maxima are observed in aqueous buffer solution (at 459 nm and 497 nm), and only one emission maximum, at 414 nm, in ethanol. These differences in the shape of the fluorescence spectra of 1,8-ANS and 2,6-ANS can be explained by the difference in geometry of the two probes, as mentioned above, and are well known in the literature.

The relative polarity of the CB[7] cavity can be determined by comparing the emission maxima of the CB[7]:1,8-ANS inclusion complexes with that of 1,8-ANS in solvents of varying polarity as listed in Table 2 for 1,8-ANS. Since the naphthalene moiety of 2,6-ANS is not included in the CB[7] cavity, its fluorescence cannot be used to determine the CB[7] cavity polarity.

Solvent	Z	E_T	ε	$\lambda_{A,max}$/nm	$\lambda_{F,max}$/nm	$\nu_{F,max}$
H_2O	94.6	63.1	78.4	350	521	19.19
K-phosph. Buff.	-	-	-	349	519	-
3:1 H_2O:MeOH	93.2	-	72.4	357	480/510	19.60
1:1 H_2O:MeOH	91.4	61.1	64.0	367	480/504	19.84
1:3 H_2O:MeOH	89.9	-	52.3	369	479/499	20.04
Methanol	83.6	55.5	32.7	372	471/494	21.23
Ethanol	79.0	51.9	24.5	372	470.5/493.6	21.25
n-butanol	77.7	50.2	20.4	375	466/494	21.46
isopropanol	76.3	-	19.9	375	462/494.5	-
acetonitrile	71.3	46.0	-	367	461/490.5	-
acetone	65.5	42.2	-	370	457/492	-
dichloromethane	64.7	41.1	-	337	433/491	-
CB[7]/phosph.buffer	-	-	-	350	469/491	21.21

Table 2. *Solvent polarity parameters; and absorption and emission maxima of 1,8-ANS in various solvents.*

Figure 19 shows a plot of $\nu_{F,max}$ ($1/\lambda_{F,max}$) of 1,8-ANS *versus* dielectric constant, ε, for the solvents listed in Table 2; a good correlation is obtained (R=0.979). Also shown in Figure 19 is the value of $\nu_{F,max}$ for CB[7] plotted on the line of best fit; this allows for determination of the dielectric constant for the CB[7] cavity, $\varepsilon = 28$. This value indicates that CB[7] has a cavity polarity similar to 50:50 methanol:ethanol. Therefore, the observed 1,8-ANS fluorescence enhancement by CB[7] and significant blue shifting in the spectrum corresponds well with the determined relative cavity polarity. Thus, the ability of CB[7] to enhance the 1,8-ANS fluorescence depends directly on the polarity experienced by 1,8-ANS molecule when incorporated within CB[7] cavity. Correlations of $\nu_{F,max}$ with other solvent polarity parameters, such as Z and E_T were also attempted; none of these was as satisfactory as the correlation obtained with solvent dielectric constant.

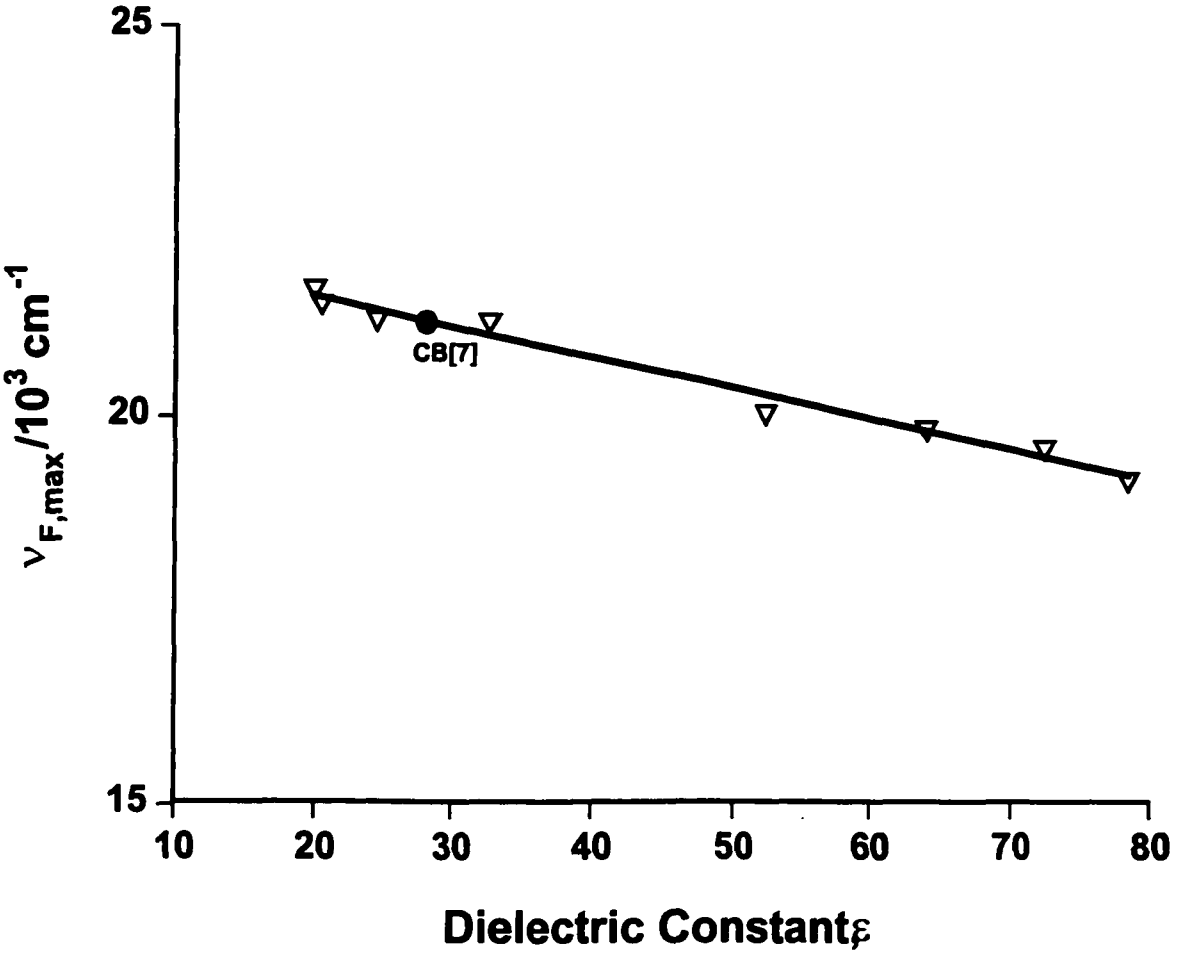

Figure 19. *Plot of fluorescence maximum $\nu_{F,max}$ vs. dielectric constant, ε, for 1,8-ANS in various solvents and aqueous CB[7] solution.*

III.3 *Thermodynamics*

In order to determine the thermodynamics of inclusion of 2,6-ANS in CB[7], the association constant K was determined for this host-guest pair at five different temperatures. This analysis was not performed for 1,8-ANS, since the complexation was not 1:1 in that case, which complicates the thermodynamic analysis.

The association constants were determined at the following five temperatures:9 ± 0.2, 19 ± 0.2, 29 ± 0.2, 39 ± 0.2, and 49 ± 0.2 °C for the CB[7]:2,6-ANS complex. The values of these association constants (averaged between at least two trials) are shown in Table 3:

Temperature/K	Association constant (K) / M^{-1}
282	584
292	567
302	498
312	366
322	227

Table 3. *Association constants at various temperatures for CB[7]:2,6-ANS complex.*

The van't Hoff plot of lnK versus 1/T for CB[7]:2,6-ANS host-guest complex is presented in Figure 20.

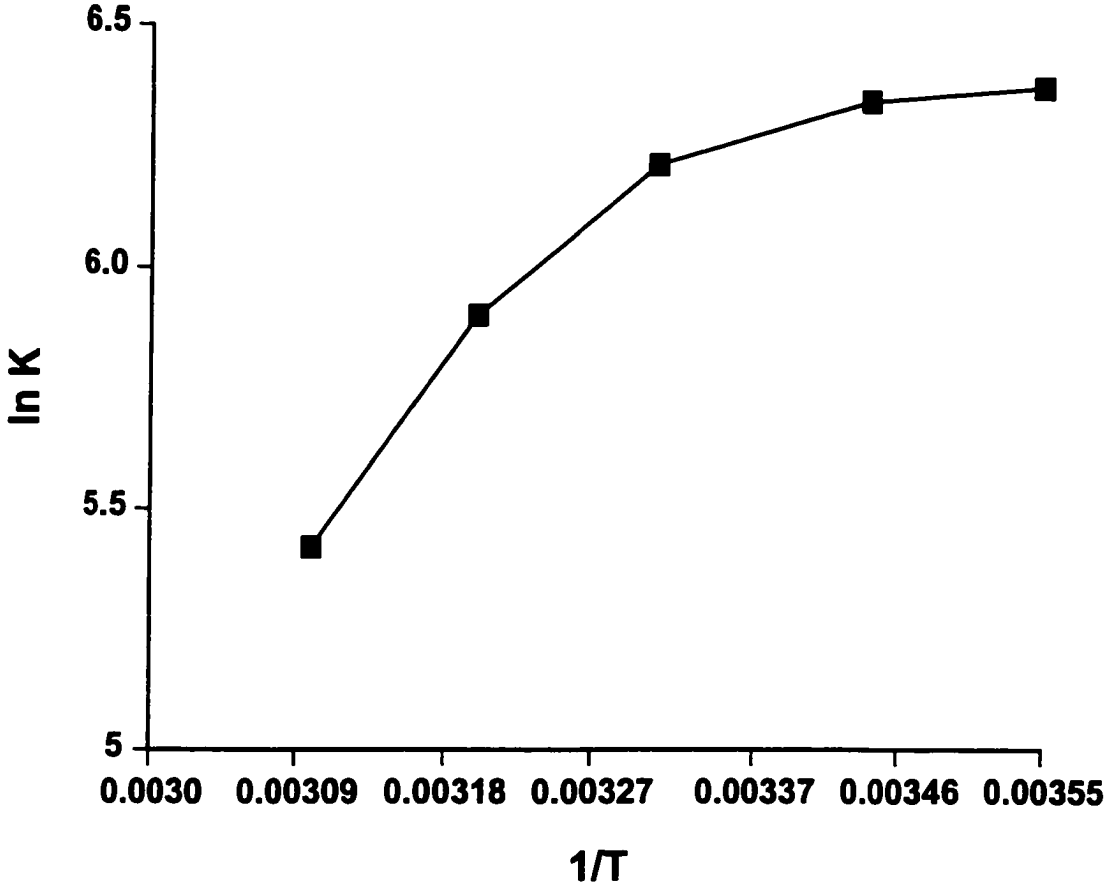

Figure 20. *Plot of lnK vs. 1/T for CB[7]:2,6-ANS complex.*

As can be seen, this plot is strongly curved. This is an interesting result, as it means that ΔH and ΔS for inclusion are not independent of T for this host-guest inclusion process, even over this relatively small temperature range used. This is in contrast to the results of most other thermodynamics studies of host-guest inclusions, for example with cyclodextrins[11], in which linear van't Hoff plots are observed. A few cases of curved plots have however been reported, including inclusion of gallic acid into β-cyclodextrin [46], formation of a porphyrin-stoppered rotaxane [47], inclusion of a protein by a crown ether [48], and a particular micelle formation process [49].

The curvature in this van't Hoff plot makes the thermodynamic analysis much more difficult. Instead of linear regression to obtain ΔH from the slope and ΔS from the y-intercept, tangents must be drawn at a particular temperature of interest, with ΔH and ΔS obtained from the slope and intercept of the tangents. Unfortunately, a graphics program which would perform such a tangent analysis was not available at this time, so the analysis was done by hand on graph paper. Two lines were drawn through temperatures 282 K and 292 K, and 312 K and 322 K, respectively to represent the tangents at the upper and lower ends of the temperature range studied. These were used to calculate the slopes and intercepts according to Equation 11. The values for ΔH^0 and ΔS^0, calculated from the slope and intercept of the first line (temperatures 282 K and 292 K) were -1.98 kJ/mol and +46.15 J/molK, respectively, while the values for ΔH^0 and ΔS^0 determined from the second line (temperatures 312 K and 322 K) were -39.91 kJ/mol and -78.65 J/molK, respectively. The value of ΔG^0 (Gibb's energy) was also calculated for each line using two different methods. In the first method, ΔG^0 was determined using the values of association constant obtained

experimentally at 292 K and 313 K from the following equation:

$$\Delta G^0 = -RT \ln K \qquad (23)$$

The second method of calculating ΔG^0 is derived from the enthalpy and entropy factors previously determined from the two above mentioned lines, using the equation:

$$\Delta G^0 = \Delta H^0 - T\Delta S^0 \qquad (24)$$

The values obtained for ΔG^0 using the both methods at the temperature of 282 K were -15.39 kJ/mol (first method) and -15.39 kJ/mol (second method), respectively, while at the temperature of 312 K they were -14.51 kJ/mol (first method) and -14.58 kJ/mol (second method). The spontaneous formation of host-guest complexes is predicted by a negative value of ΔG^0. The degree to which a complex is formed spontaneously though depends on how large the negative value of ΔG^0 is. The negative value of this quantity is facilitated both by a negative value for the enthalpy and a positive value for the entropy of the system. The values of ΔG^0, calculated from both methods were almost identical, indicating that the calculations of ΔH^0 and ΔS^0 from the lines drawn at the two ends of the curvature were quite reliable.

The two values of ΔH^0 obtained from the slopes of two lines drawn through temperatures 282K and 292K, and 312K and 322K, respectively are both negative. However, the enthalpy is a measure how efficiently the guest and host molecules interact

to form the inclusion complex. Thus, complexes with a more negative ΔH^0 value interact with each other more strongly, forming a more stable and thermodynamically favourable complex. As the results show, the binding of the 2,6-ANS guest is less efficient at the lower temperatures than at higher, resulting in a smaller negative ΔH^0 value as compared with that calculated at the higher temperature. It is interesting to note that the entropy associated with the complex formation between 2,6-ANS and CB[7] is positive at lower temperatures (46.15 J/mol K at 282 K), while negative at higher temperatures (-78.65 J/mol K at 322 K) The negativity of the ΔS^0 value at higher temperatures suggests that more order is created within the system upon increasing the temperature. Usually, when the host-guest formation process is considered, entropy should be always positive due to the fact that upon inclusion of the guest into the host cavity, the water molecules occupying the host cavity prior the complexation are forced out from the cavity resulting in an increase of a number of species present in the system (solution), therefore giving a positive value of ΔS^0. A possible explanation for the negative value of ΔS^0 at higher temperatures can be that the cavity of the CB[7] is expanded due to the bond stretching, resulting in the inclusion of water molecules from the solution even in the complex.

The more negative ΔG^0 value at the lower temperature, 282 K, indicates that formation of CB[7]:2,6-ANS host-guest complex is more spontaneous, with positive entropy value, but is less efficient due to a less negative enthalpy value compared to all these quantities at the higher temperature. Results indicate that the more negative ΔG^0 value observed at the lower temperature is mainly a result of the large positive entropy value, while the observation of the decreased ΔG^0 value at higher temperature is mainly due to the

negative entropy value. A comparison of the values of ΔH^0, ΔS^0, and ΔG^0 calculated at two different temperatures, 282 K and 322 K, suggests the existence of the relationship referred to as entropy-enthalpy compensation.[11] This purely empirical relationship proposes that for host-guest systems in which the enthalpy is quite high, a decrease in entropy is observed as a compensatory mechanism. According to the values derived from this compensatory relationship, host-guest inclusion which is favoured by a large enthalpic change will be less favoured by a small, or even negative entropic change. This is exactly what was observed here, where the ΔH^0 value of -1.92kJ/mol at 282 K was increased to - 39.91 kJ/mol at 322 K, accompanied by the change in entropy from positive value of 46.15 J/mol K to negative value of -78.65 J/mol K, respectively. Although no direct relationship between variations in entropy and enthalpy can be arrived at by the fundamentals of thermodynamics, an empirical correlation between the two has long been seen to exist.[11] As shown in literature[11], this entropy-enthalpy compensation can be represented graphically when ΔH^0 and $T\Delta S^0$ are plotted. The result, if the entropy-enthalpy relationship is real, is a straight line. Such a plot is well known and well studied by incorporating the ΔH^0 and $T\Delta S^0$ relationships for numerous cyclodextrins. [11] In fact, the values of ΔH^0 and ΔS^0 obtained in this project fall on the same correlation line as that given in reference 11 for cyclodextrin inclusion, suggesting that this enthalpy-entropy compensation phenomenon is universal for all host-guest inclusion processes.

As mentioned previously, the plot of lnK versus 1/T for the complexation of 2,6-ANS with CB[7] is strongly curved, meaning that ΔH and ΔS for inclusion are not independent of T, even over this relatively small temperature range used. The curvature in

the van't Hoff plot indicates that there is a change in the total heat capacity, Cp, for the inclusion process, i.e.,Cp of the complex is different from the total Cp of the free guest and host.[11] In other words, there is an non-zero ΔCp for this inclusion process. This will occur if there is a significant conformation change in either the guest or host upon complexation; this was reported to be the case in all above mentioned reports of non-linear van't Hoff plots. [46-49] In the present case the host CB[7] is extremely rigid , so it is difficult to explain the non-zero ΔCp based on changes to the host. Therefore, there must be significant conformational changes in the 2,6-ANS guest. However significant changes in 2,6-ANS are also difficult to imagine. Such changes were not observed for inclusions of 2,6-ANS in natural and modified β-cyclodextrins, for example[50]. It may be possible to use molecular modelling to further investigate this interesting observation. Further work on the thermodynamics studies of these inclusion complexes will be carried out by this research group in the future.

III.4 *Time-resolved Fluorescence Results*

Time-resolved fluorescence was also applied to the host-guest complexes of 2,6-ANS with CB[7]. In the literature, the observed fluorescence decay curves are often fit to a two-exponential decay function, where one lifetime represents the free guest and the other the complexed guest. Thus, these components can be resolved according to the equation:[51]

$$I_F(t) = A_1 \exp(-t/\tau_1) + A_2 \exp(-t/\tau_2) \qquad (25)$$

where A_1 and A_2 are preexponential factors, giving the relative weights of the two components, and τ_1 and τ_2 are the lifetimes of the free and bound guest.

The degree of interaction between the fluorophore and CB[7] can be judged from the relative size of the A parameters. Since each A is related to the concentration[51] of the species, the ratio of the A_2/A_1 will show the relative concentration of the two components in the mixture. In the case of mixture of 2,6-ANS and CB[7], components A_1 and A_2 are free and complexed 2,6-ANS, respectively. If this ratio increases with increasing the CB[7] concentration, then some information about the formation of the inclusion complex can be gained. The lifetime of the complexed and free 2,6-ANS is an indicator of the fluorophore's environment. Differences in lifetimes can generally be attributed to changes in the deactivation pathways of the excited state or changes in the interaction of the excited state with the surroundings in solution as compared with within the cavity.

One of the goals of this project was to determine if the equilibrium association constant for the complexation of 2,6-ANS with CB[7] could be determined using the results from the lifetime measurements, for example, using the ratios of the preexponential factors for the two exponential decays. Table 4 gives the values of A_2/A_1 (for two exponential fit), and τ/τ_0 (for one exponential fit) for 2,6-ANS with CB[7].

[CB[7]]/mM	τ/ns	τ/τ_0	τ_1/ns	τ_2/ns	A_1	A_2	A_2/A_1
0	0.809	1.0	0.319	2.529	0.904	0.026	0.028
2	3.257	4.02	1.710	3.701	0.106	0.159	1.500
4	3.544	4.38	2.628	5.407	0.249	0.076	0.305
6	3.740	4.62	2.858	5.790	0.255	0.059	0.213
8	4.100	5.06	2.831	6.280	0.179	0.031	0.173
10	4.109	5.07	3.194	7.673	0.178	0.016	0.090

Table 4. *Lifetime data for 2,6-ANS with various concentrations of CB[7].*

Previous studies [51-53] had reported that the equilibrium constant, K, can be determined by plotting A_2/A_1 as a function of host concentration. Figure 21 shows the graph of A_2/A_1 plotted as a function of CB[7] for 2,6-ANS. As can be seen, there is no smooth correlation.

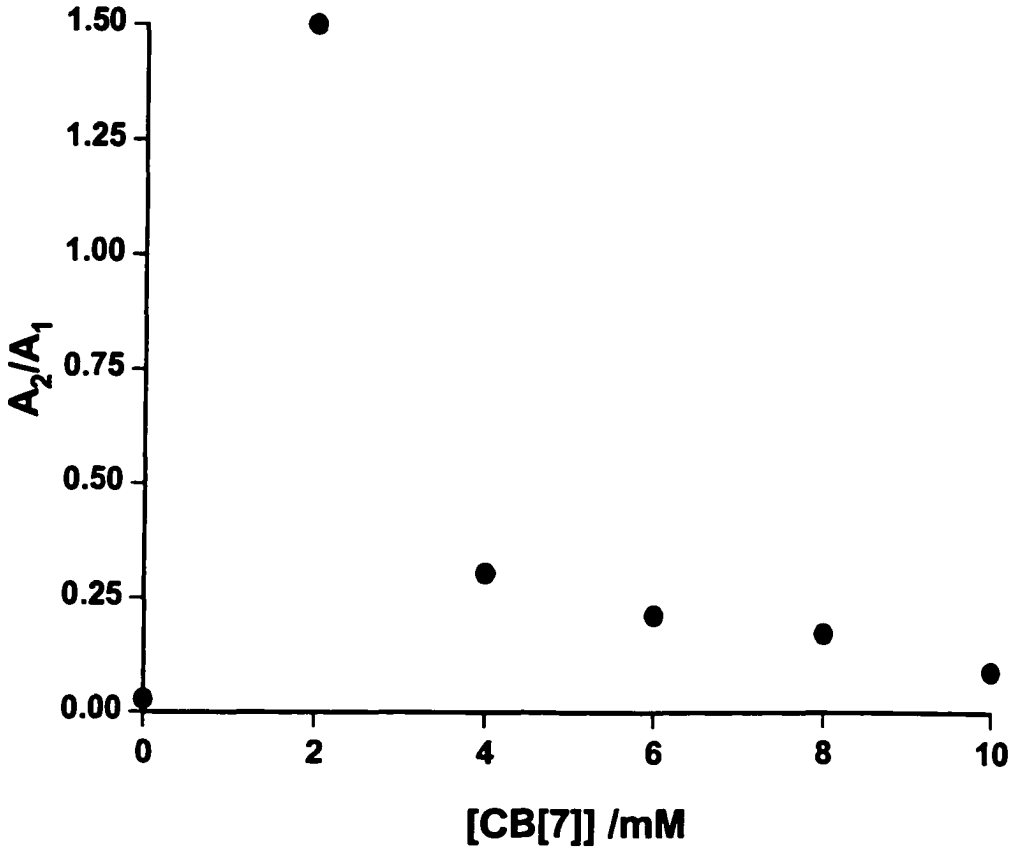

Figure 21. *Plot of A_2/A_1 plotted as a function of CB[7] for 2,6-ANS.*

The ratio of the fluorescence lifetimes, τ/τ_0, where τ is the lifetime of complexed 2,6-ANS molecule, and τ_0 is its lifetime in the absence of CB[7] (assuming one exponential decay), as a function of CB[7] concentration was also plotted as shown in Figure 22. These data were used to obtain the association constant using a non-linear regression program; the analysis indicated that the information obtained about the K value can not be used because the K values obtained were huge compared to those calculated using the steady-state fluorescence spectroscopy technique. It is also important to mention that the lifetime of the inclusion complex in no way indicates the strength of the equilibrium constant, K, between the host and guest molecules. A longer lifetime of one complex compared to an other cannot necessarily be associated with a larger equilibrium constant.

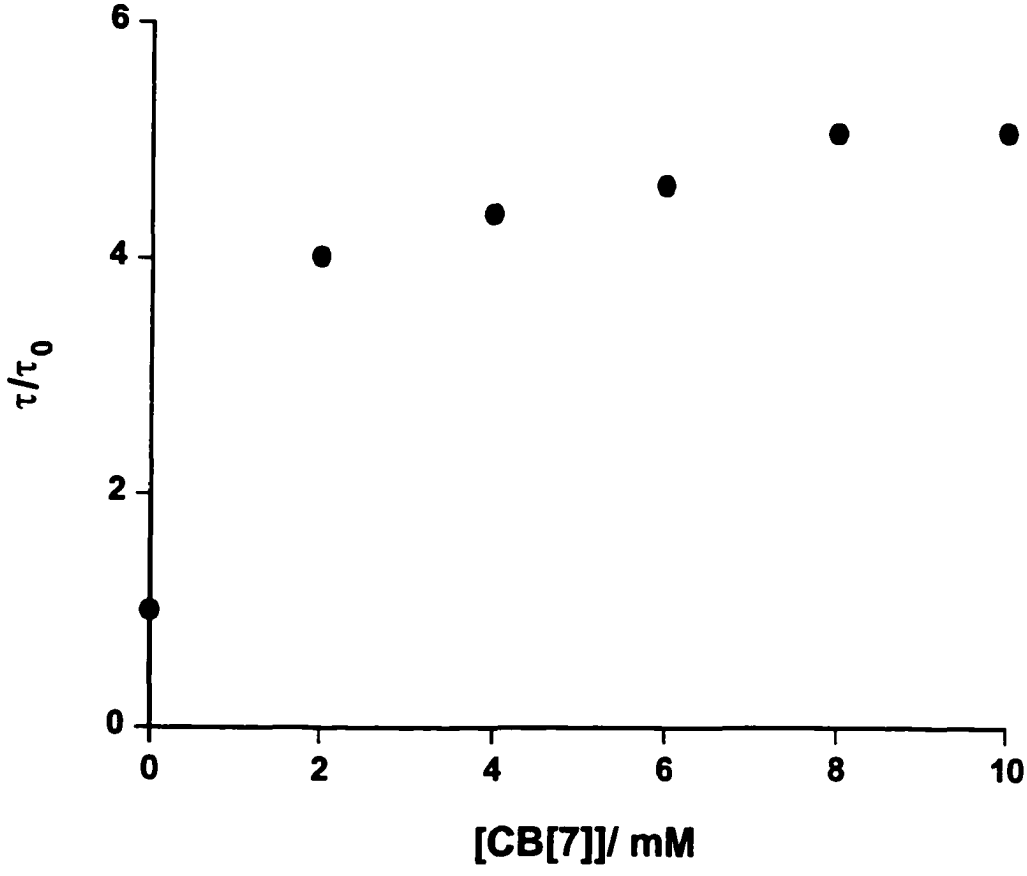

Figure 22. *Plot of τ/τ_0 plotted as a function of CB[7] for 2,6-ANS.*

In the studies previously mentioned[51-53], the two preexponential factors obtained (in the presence of the host molecule) represented the free guest molecule, having the shorter lifetime, and the complexed guest molecule with the longer lifetime. When the host molecule concentration is increased, the ratio of preexponential factors should change; A_1 should decrease with increasing the host concentration, while A_2 should increase with the increase of the host concentration. Therefore, the ratio of preexponental factors can be used to determine the association constants. If only one type of complex is formed, then the plot of A_2/A_1 versus host concentration should be the straight line. As can be seen from both Table 3 and Figure 21, in the case of 2,6-ANS, the ratio of preexponential factors with the change in CB[7] concentration is not changing as expected.

Although the lifetimes and preexponential factors were not useful in obtaining the values of the association constants, K, useful information was still obtainable from the lifetime results. As mentioned previously, the χ^2 value is an indication of how good the exponential fit is to the actual decay. The closer its value is to unity, the better fit is to the actual fluorescence decay. In the case of 2,6-ANS, the free guest has such a low fluorescence and short lifetime that it does not contribute to the measured decay in the presence of the host. If only one type of complex is formed between 2,6-ANS and CB[7] molecules, then the solution will have a single exponential decay, giving one value for the fluorescence lifetime. If upon complexation with CB[7], 2,6-ANS molecules experience several distinct environments, or form several types of complexes with CB[7] or they are even complexed to different degrees by the host, then multiple exponential decay constants will be obtained as well as a fluorescence lifetime for each of the different emitting species.

A solution of 2,6-ANS in the absence of CB[7] had very weak fluorescence, therefore the fluorescence decay of 2,6-ANS was short-lived and had a lifetime of only 0.319 ns. The decay was a single exponential with a χ^2 value of 1.07. However in the presence of 10 mM CB[7] (Figure 23), the fluorescence lifetime increased to 7.67 ns, and it was a two exponential decay, with χ^2 value of 0.80. Also, the fluorescence decay of 2,6-ANS in ethanol was best described by one exponential fit, since all ANS molecules were experiencing a homogeneous environment.

In this study of the inclusion complexes of CB[7], it was shown 2,6-ANS forms 1:1 host-guest inclusion complexes with CB[7], i.e. one 2,6-ANS molecule is complexed with one CB[7] molecule. The fluorescence lifetime of 2,6-ANS in the absence of CB[7] is very small, but when 10 mM CB[7] was added, the fluorescence lifetime of 2,6-ANS increased dramatically. Two long-lived components are observed upon the addition of CB[7]. The magnitude of the lifetime of the included 2,6-ANS is a strong indication that an inclusion complex is formed. For such a change in lifetimes, a substantial change in the environment of the fluorophore is implied. The cavity of CB[7] provides 2,6-ANS with less polar environment, thereby resulting in an increase in lifetime. The fluorescence decay curve of 2,6-ANS molecule is best described by a two exponential fit decay, indicating that two different types of 1:1 inclusion complexes are formed, since the lifetime of the free 2,6-ANS is much shorter then either of the two fit lifetimes of ca. 3 and 7 ns. These two types of complex could differ in the way that the 2,6-ANS molecule is incorporated into the CB[7] cavity or simply in the degree of penetration, or relative orientation between guest and host.

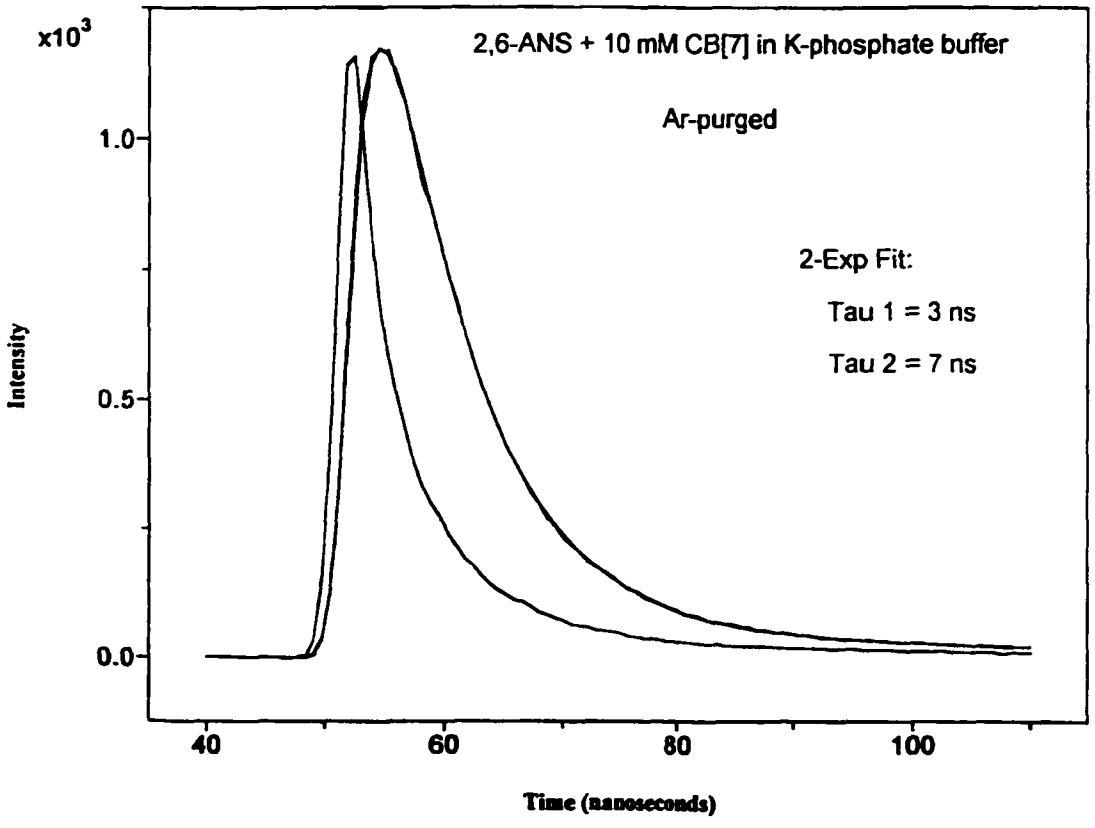

Figure 23. *Fluorescence decay curve of 2,6-ANS with 10mM CB[7].*

In the literature, when double exponentional decays are fitted, it is always assumed that the short-lived species is due to the free guest molecules while the long-lived component arises from the complexed guest molecules. Most inclusion complex studies are based on this assumption. But statistically, upon complexation with the host, guest molecules can experience several distinct environments or form several types of complexes. They can be even complexed to different degrees by the host. This would definitely result in multiple exponential decay constants as well as a fluorescence lifetime for each of the different emitting species. These results call into question the interpretation of observed double exponential fluorescence decay for host-guest inclusion complexes in the literature as arising from the free and complexed guest. It is clear from these results that multiple exponential decay can arise just from the complexes themselves. In other words, host-guest inclusion complexes are likely to be heterogeneous in nature. Further work on the application of time-resolved fluorescence to inclusion complexes will be carried out by this research group in the future. For example, it may be necessary to fit the decay curves of host-guest inclusion complexes using fluorescence lifetime distribution analysis methods [54,55], which allow for a whole range of lifetimes instead of the maximum of four discrete lifetimes allowed by Equation 22. There are only a few examples in the literature of the application of fluorescence lifetime distribution analysis to the decay of a host-guest inclusion complex, such as that of Bright *et al.* [56], who found evidence for lifetime distributions in the case of various ANS probes in β-cyclodextrin.

IV. *INCLUSION COMPLEXES OF CALIXARENES*

Calixarenes represent another important type of host with a relatively non-polar internal cavity. This cavity is quite different from that of cyclodextrin and cucurbituril, however, because it is lined by π-electrons. The commercial availability of water-soluble *p*-sulfonic calixarenes opens up the possibility of studying these hosts using fluorescence enhancement of a polarity-sensitive fluorescent probe as guest. To this end, a wide range of fluorescent probes were tested in an attempt to observe fluorescence enhancement of a guest in aqueous solutions, which has never been previously observed with *p*-sulfonic calixarenes.

As previously mentioned, during the course of this project, two different types of powder (white and gray) of both *p*-sulfonic calix[4]arene and *p*-sulfonic calix[6]arene were purchased, which significantly affected our spectroscopic studies of inclusion complexes of these calixarenes. The white samples of *p*-sulfonic calix[4]arene and *p*-sulfonic calix[6]arene were of high quality absorbing significantly only up to 310 nm. The gray powder though was very impure, showing very high absorbance at wavelengths even up to 550 nm. Therefore, the probes with lower absorption maxima (2,6-ANS, and Dansyl Lysine as well as lanthanides) could be used in the fluorescence studies only with the white *p*-sulfonic calix[4]arene and *p*-sulfonic calix[6]arene, while probes with higher values of absorbance maxima such as Nile Red, Nile Blue, Neutral Red, and Resorufin as well as lanthanides could be used with the gray calixarenes. It is also important to mention that both of these calixarenes showed significant fluorescence (presumably from impurities), therefore in the

calculation of the fluorescence enhancement, F/F_0, of each probe, the integrated area of the fluorescence spectrum of the calixarene itself was subtracted from the integrated area of the fluorescence spectrum of the probe in the presence of the calixarene of interest.

IV.1 *ANS as Guest*

2,6-ANS was the first probe used as a guest molecule with both *p*-sulfonic calix[4]arene and *p*-sulfonic calix[6]arene as hosts. As can be seen from Table 5, decreased fluorescence was observed for 2,6-ANS by both *p*-sulfonic calix[4]arene and *p*-sulfonic calix[6]arene. In addition, no significant change in the absorption spectrum of 2,6-ANS was observed upon the addition of calixarene of interest.

Solution	A_{350}	$\lambda_{F,max}$/nm	F/Fo
10mM 4SCA/H_2O	0.0162	422	-
20mM 4SCA/H_2O	0.0811	427	-
2,6 ANS/H_2O	0.2844	479	1.0
10mM 4SCA/H_2O/2,6ANS	0.2477	472	0.78
20mM 4SCA/H_2O/2,6ANS	0.2067	457	0.38
10mM 6SCA/H_2O	0.0238	430	-
10mM 6SCA/H_2O/2,6ANS	0.5169	471	0.78

Table 5. *Absorbance and fluorescence parameters of 2,6 ANS with 4SCA and 6SCA in water.*

1,8-ANS was also studied as a guest for these calixarenes, with the same result: no changes in the absorption spectrum but a significant decrease was observed in the fluorescence spectrum.

IV.2 *Dansyl Lysine as Guest*

The next probe used was Dansyl Lysine, the structure of which is shown in Figure 9, structure **2**. As can be seen from Table 6, the fluorescence measurements of Dansyl Lysine with *p*-sulfonic calix[4]arene showed no enhancement of the probe fluorescence; in fact, decreased fluorescence is again observed. In contrast to 2,6-ANS, absorbance measurements of Dansyl Lysine with *p*-sulfonic calix[4]arene provided very interesting results. A decrease in the intensity of the absorption band at 350 nm, and an increase of another absorption band at 290 nm were observed upon increasing the concentration of *p*-sulfonic calix[4]arene (4SCA), as shown in Figure 24. Furthermore, an isosbestic point at 321 nm was observed indicating 1:1 equilibrium between the Dansyl Lysine and calixarene. All these absorbance parameters are shown in Table 7. Also, the addition of increasing amounts of *p*-sulfonic calix[4]arene to aqueous solutions of Dansyl Lysine, resulted in a small bathochromic shift of the wavelength of the maximum absorption (Figure 24).

Solution	A_{350}	$\lambda_{F,max}$ /nm	F/F_0
Dansyl Lysine in H_2O	0.2626	564	1.0
0.05mM 4SCA in DL/H_2O	0.1274	566	0.48
0.1mM 4SCA in DL/H_2O	0.0719	564	0.33
0.5mM 4SCA in DL/H_2O	0.0184	553	0.035
1.0mM 4SCA in DL/H_2O	0.0204	-	0.031
2.0mM 4SCA in DL/H_2O	0.0168	436	0.025
5.0mM 4SCA in DL/H_2O	0.0269	424	0.035
10.0mM 4SCA in DL/H_2O	0.0296	433	0.050
0.05mM 4SCA in H_2O	0.0107	-	0.009
0.1mM 4SCA in H_2O	0.0144	-	0.015
0.5mM 4SCA in H_2O	0.0107	407	0.010
1.0mM 4SCA in H_2O	0.0152	410	0.017
2.0mM 4SCA in H_2O	0.0153	414	0.023
5.0mM 4SCA in H_2O	0.0205	433	0.038
10mM 4SCA in H_2O	0.0310	440	0.072

Table 6. *Absorbance and fluorescence parameters of Dansyl Lysine with and without 4SCA.*

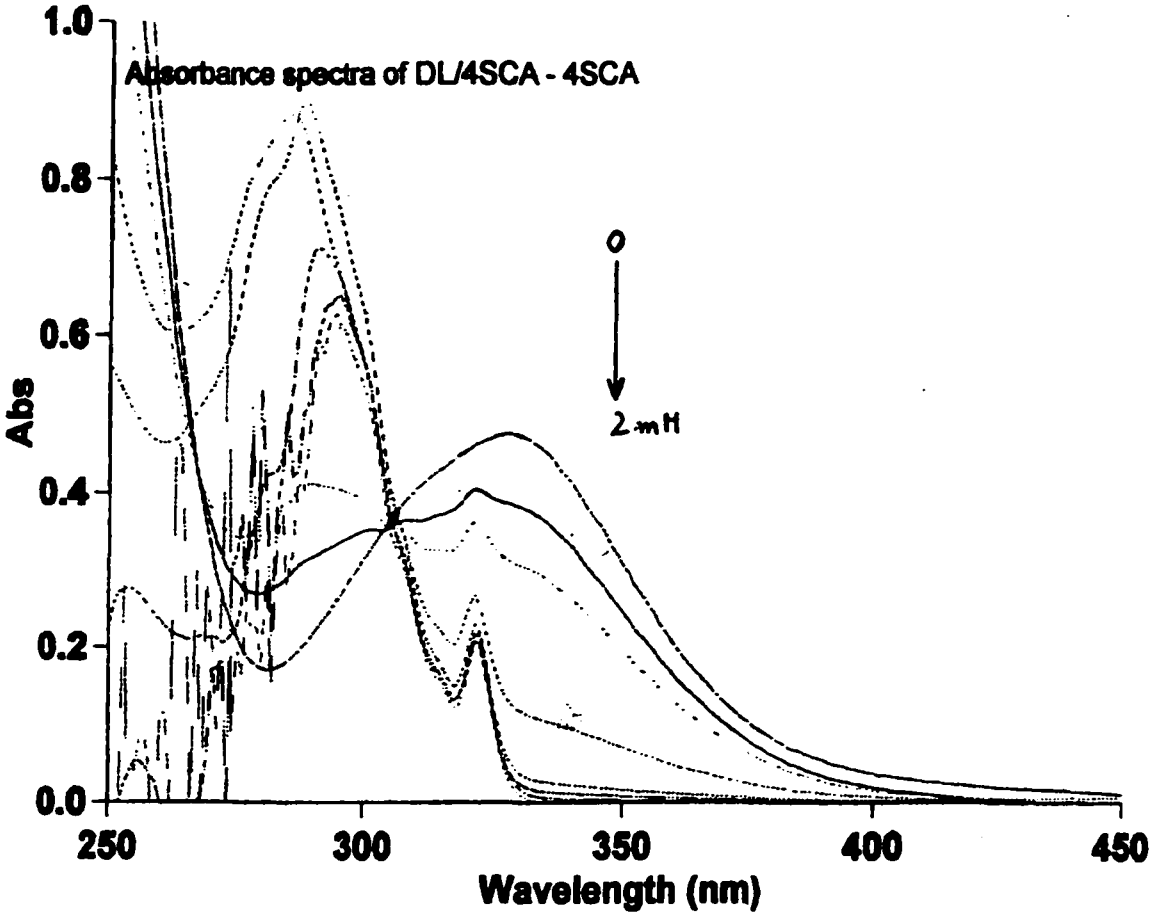

Figure 24. *Absorbance spectra of Dansyl Lysine with p-sulfonic calix[4]arene in aqueous solution.*

Solution	A_{350}	A_{321}	A_{350}/DL/4SCA - A_{350}/4SCA	A_{321}/DL/4SCA - A_{321}/4SCA	A_{290}/DL/4SCA - A_{290}/4SCA
DL/H_2O	0.3088	0.4740	0.3088	0.4740	-
0.02mM 4SCA/DL/H2O	0.2564	0.3974	0.2466	0.4039	-
0.02mM 4SCA/H2O	0.0098	0.0120			
0.05mM 4SCA/DL/H2O	0.2105	0.3790	0.1978	0.3630	0.4094
0.05mM 4SCA/H2O	0.0127	0.0490			
0.1mM 4SCA/DL/H2O	0.0882	0.2780	0.0790	0.2666	0.8817
0.1mM 4SCA/H2O	0.0092	0.0150			
0.25mM 4SCA/DL/H2O	0.0269	0.2323	0.0166	0.2290	0.9030
0.25mM 4SCA/H2O	0.0103	0.0187			
0.5mM 4SCA/DL/H2O	0.0211	0.2318	0.0073	0.2109	0.7107
0.5mM 4SCA/H2O	0.0138	0.0185			
1.0mM 4SCA/DL/H2O	0.0145	0.2337	0.0015	0.2168	0.6473
1.0mM 4SCA/H2O	0.0130	0.0197			
2.0mM 4SCA/DL/H2O	0.0143	0.2340	-0.0007	0.2070	0.6268
2.0mM 4SCA/H2O	0.0150	0.0206			

Table 7. *Absorbance parameters of DL/4SCA and 4SCA in H_2O.*

The changes observed in absorbance as a function of calixarene concentration can be related to the corresponding association equilibrium constant, K, as

$$\Delta A = K \Delta \varepsilon \text{ [calixarene]} / 1 + K\text{[calixarene]} \qquad (26)$$

The resulting plot of ΔA as a function of *p*-sulfonic calix[4]arene concentration is non-linear. Non-linear fitting of these data according to above equation leads to the association constant, K. However, the results obtained from this fit were not satisfactory. Moreover, the double reciprocal plot was not linear.

IV.3 *Nile Red as Guest*

As mentioned previously in the experimental section, two different methods were used for preparing the solutions of Nile Red and *p*-sulfonic calix[4]arene and *p*-sulfonic calix[6]arene. In Method A, where solutions were prepared by adding both Nile Red and calixarene of interest initially, and then filtering the undissolved Nile Red, an interesting observation was made, which indicated complex formation between the probe and host. When Nile Red and either *p*-sulfonic calix[4]arene or *p*-sulfonic calix[6]arene were mixed, the colour of the solution changed from brown to green 24 hours after mixing. Upon changing from Method A to Method B, where, as mentioned previously, the stock solution of Nile Red was prepared first in the absence of calixarene, and then undissolved Nile Red was filtered, no significant change either in fluorescence intensity or in the colour of solution

by studied calixarene was observed. Therefore, a decrease in the fluorescence intensity of Nile Red was observed in both methods, while the colour of solution upon the addition of calixarene was observable only in method A. However, the fluorescence and absorption spectra of Nile Red were shifted to the higher wavelengths upon the addition of calixarene in both cases, suggesting the formation of a complex with the calixarene.

IV.4 *Lanthanides as Guests*

Lanthanide ions show strong luminescence, which sometimes can be enhanced upon complexation by supramolecular hosts. However, when lanthanides (Eu(III) and Sm(III)) were used as guest molecules with these calixarenes, again no enhancement of either lanthanide fluorescence was observed. In order for lanthanides to show significant fluorescence enhancement, the host molecule must have a lowest excited state sufficiently high enough in energy for energy-transfer to lanthanide ions to occur. In other words, fluorescence of the metal ion occurs upon light absorption by the ligand (host) followed by ligand-to-metal energy transfer.[57] With the calixarenes used in this project, *p*-sulfonic calix[4]arene and *p*-sulfonic calix[6]arene, that could not be achieved. In our attempt to study the fluorescence of lanthanides upon mixing with the calixarene of interest, however, an unexpected thing happened. Upon mixing 50 mM *p*-sulfonic calix[4]arene with 0.1 M $EuCl_3$ in water, white crystals were obtained. The fluorescence spectrum of these crystals proved the presence of Eu(III). Also crystals of the same complex were prepared by the diffusion method, where solutions of above mentioned concentrations were allowed to mix

slowly by diffusion in two connected test tubes. Unfortunately, crystals of very poor quality were obtained using this method, and therefore could not be analysed by crystallography methods. Thus, it is not clear whether a host-guest inclusion solid was formed. The emission fluorescence spectra of these fluorescent crystals, as well as Eu(III) itself, are shown in Figure 25.

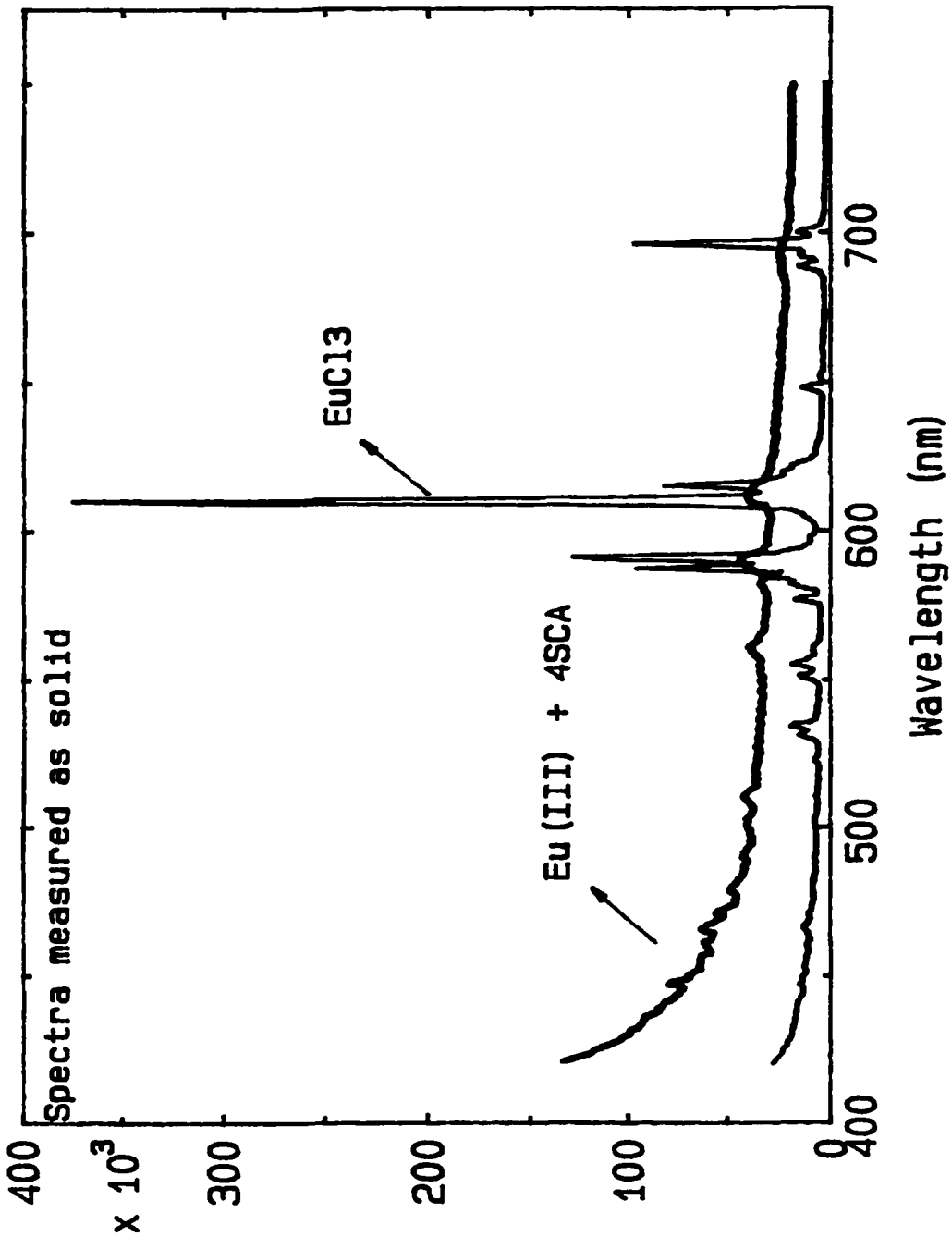

Figure 25. *Fluorescence spectra of Eu(III) and p-sulfonic calix[4]arene crystals.*

IV.5 *Other Probes as Guests*

When the probes Nile Blue, Neutral Red, and Resorufin were used with the gray *p*-sulfonic calix[4]arene and *p*-sulfonic calix[6]arene, the same results were obtained as that for 2,6-ANS and Dansyl Lysine, namely a decrease in the fluorescence of each above mentioned probe is observed upon addition of the calixarene of interest. No significant changes in the absorption spectra of these probes were observed.

IV.6 *Fluorescence Studies of Calixarene Inclusion Complexes in the Literature*

As mentioned previously, there have been relatively few studies of the effects of encapsulation of sulfonic water soluble calixarene on the fluorescence of incorporated guest molecules. In our attempt to study the inclusion complexes of water soluble calixarenes, decreased fluorescence of the probe molecule used was observed in every single case. By contrast, Shinkai and co-workers reported fluorescence studies on inclusion complexes of sulfonic and phosphono derivatives of calix[6]arene with aminonaphthalene derivatives[34], pyrene[35] and 1,8-ANS as fluorescent probes[33].

In the case when 1,8-ANS was used as fluorescent guest molecule, two different types of water soluble calix[6]arene were used, cationic and anionic.[33] Both of these calixarenes had methoxy groups at the lower rim instead of OH groups. Using the cationic calix[6]arene they reported that the fluorescence intensity of 1,8-ANS was increased, supporting the fact that 1,8-ANS is included in the hydrophobic cavity of this calixarene. In

contrast, the authors reported that the fluorescence intensity of the same probe was scarcely increased by the addition of anionic calix[6]arene. Since the 1,8-ANS molecule is an anion, this kind of behaviour could be explained by the fact that the electrostatic repulsion overcomes the hydrophobic interaction. Also, using the cationic and neutral probes with these two types of water soluble calixarenes, they were able to show that hydrophobic forces are generally operative for complex formation in aqueous system, but the selectivity is crucially governed by the electrostatic forces. As a result of the important role of electrostatic forces in the formation of the inclusion complexes of water soluble calixarenes, a shift to longer wavelengths (red shift) in both absorbance and fluorescence spectra of the fluorophores is usually observed. For example, Shinkai showed that absorbance spectrum of Phenol Blue in the presence of *p*-sulfonic calix[6]arene shifts to longer wavelength. They explained this phenomenon as a result of the fact that the six sulfonate groups lining the edge of the calix[6]arene are capable of stabilizing the excited-state structure of probe through the electrostatic interaction, therefore leading to the unusual red shift.[35] Also, Shinkai and co-workers[36] reported a decrease in the fluorescence intensity of pyrene fluorescence upon addition of water soluble sulfonic calix[6]arene, where at the lower rim of this calixarene the OH group hydrogen was substituted by a methyl group. This phenomenon was explained as the result of the quenching effect of the calixarene π-system. Barra and Tao[37] reported association equilibrium constants and thermodynamic parameters for complexation between N,N-dimethylindoaniline and *p*-sulfonic calix[n]arenes (n=4,6, and 8) in aqueous solution by UV-VIS spectroscopy. In each case an increase in absorption intensity for N,N-dimethylindoaniline was observed. It was shown that the association

equilibrium constants and the thermodynamic parameters for complexation depend on the size of the calixarene cavity, and particularly, on the type of the substituent on the lower rim of the host molecule. Similarly, Shinkai in his studies of inclusion complexes of water soluble sulfonic calixarene with a variety of probes established that the complexation of the probe with *p*-sulfonic calix[4]arene it is due to the electrostatic force, whereas that with *p*-sulfonic calix[6]arene and *p*-sulfonic calix[8]arene is due to the hydrophobic force, simply because of the larger cavities compared to that of *p*-sulfonic calix[4]arene. He also reported that the cation-π interaction can compete effectively with the hydrophobic interaction. This explanation states that in acidic medium some OH groups at the lower rim are protonated, while in the neutral medium some OH groups are deprotonated, thus changing the electron density in the benzene π-systems of calixarene.

IV.7 *Discussion*

As seen above, each probe used in this project showed decreased fluorescence upon addition of the calixarene of interest, whereas inclusion of the probe within the less polar calixarene cavity would be expected to result in fluorescence enhancement. A possible explanation for the decreased fluorescence of 2,6-ANS by both *p*-sulfonic calix[4]arene and *p*-sulfonic calix[6]arene is as follows: The structures and sizes of both host and guest molecules indicate that probably only the phenyl moiety of the 2,6-ANS molecule (structure shown in Figure 5) is included within the cavity of calixarene. In addition, the SO_3^- group is located on the naphthalene part of the molecule, causing repulsion with the SO_3^- and O^-

groups of the calixarene, which therefore prevents the inclusion of naphthalene part of the 2,6-ANS molecule. When the phenyl moiety is included within the host cavity, there is a change in the density of benzene π-systems of both calixarene and the included phenyl moiety of the 2,6-ANS molecule, induced by dissociation of the OH groups, thereby resulting in a decrease of the 2,6-ANS fluorescence. Another explanation for the decreased fluorescence of 2,6-ANS molecule involves the fact that the 2,6-ANS molecule is an anion as are both calixarenes used, so the electrostatic repulsion might overcome the hydrophobic interaction, as Shinkai reported in his studies of inclusion complexes of 1,8-ANS molecule with cationic and anionic water soluble calixarenes.

Looking at the structure of the Dansyl Lysine fluorophore, the observed decrease in its fluorescence might be explained by the fact that the carboxyl group is probably deprotonated in aqueous medium causing the repulsion between this part of fluorophore and the anionic calixarene. At the same time the amino group can be protonated and therefore can interact with the anionic SO_3^- and deprotonated OH groups. The fluorescence studies of Dansyl Lysine were performed only with *p*-sulfonic calix[4]arene, and therefore the cavity size of this calixarene is not big enough to accept the whole part of the naphthalene ring of Dansyl Lysine molecule. Therefore, the change in the absorption spectra as well as decreased fluorescence of Dansyl Lysine upon addition of *p*-sulfonic calix[4]arene can be only explained assuming that interaction between the amino part of the probe molecule and SO_3^- and O^- groups cause some electron transfer to the naphthalene part of the probe, which results in decreased fluorescence. As can be seen from Figure 9, Nile Red, Neutral Red, Nile Blue and Resorufin probes have very similar molecular structures. The cavity sizes of

both calixarenes definitely are not big enough to accept the whole probe within their cavities. But Neutral Red, and Nile Blue, unlike Nile Red are positive probe molecules. As mentioned previously, the fluorescence intensity of these dyes decreased markedly upon the addition of *p*-sulfonic calix[4]arene and *p*-sulfonic calix[6]arene. The electrostatic interaction between the positively charged dye molecules and the negatively charged substituent groups in the calixarene ring, as well as the hydrogen bonding and restricted the internal rotation should lead to the fluorescence enhancement. In contrast, opposite behaviour was observed for each probe molecule.

From the bathochromic shift and the decrease in fluorescence intensity, it can be concluded that these four probes formed host-guest inclusion complexes with these calixarenes. Although there is no direct evidence for the inclusion by calixarene hosts, the possibility of the formation of an "external-type" complexes can not be ruled out. Since all these probes are aromatic, there is also the possibility of interaction between the π-electrons of the probe with the π-electrons of the calixarene cavity, which can result in an increased rate of non-radiative decay, therefore causing the observed decrease in the fluorescence intensity. For example, Liu and co-workers [58] studied the inclusion complexation of Acridine Red dye by calixarenesulfonates, where they also observed opposite fluorescence behaviour (decreased fluorescence of the probe upon complexation with the calixarene host). They also showed that the fluorescence intensity of Acridine Red was enhanced upon the addition of butylated *p*-sulfonic calix[6]arene as compared with *p*-sulfonic calix[6]arene. This phenomenon was explained as a result of the alkylation on the lower rim of the parent *p*-sulfonic calix[6]arene which enlarges the hydrophobic cavity of the calixarene ring which

therefore resulted in fluorescence enhancement.

In spite of the diversity of calixarene structures available, the literature contains only a limited number of reports describing well-characterized complexation by calixarene hosts in the solution phase. Many aspects of calixarene and their inclusion abilities are still not very clear. A variety of effects, such as conformation properties, functionalization of its aromatic rings, π-systems and the complexity of the structure, should be taken into consideration when studying them. They are able to recognize organic molecules on the basis of their sizes and shapes. In this context the conformational properties of calixarenes are of particular relevance, since they are not completely rigid molecules, and their shape and flexibility can also be varied by changing the solvent, temperature, and by further functionalization. Four of the most common conformations of calixarenes are the cone, partial cone, 1,2-alternate and 1,3-alternate. As the number of phenol units is increased, the number of possible conformations of calix[n]arene becomes much higher. Also, an important role is played in the complexation of calixarenes, particularly water soluble sulfonic calixarenes, by the phenolic hydroxy groups which are, as mentioned previously, protonated in acidic medium (pH=0.4), while deprotonated in neutral medium (pH=7.3). Also, the big concern in the studies of the inclusion complexes of calixarenes by fluorescence spectroscopy is the fact that they are fluorescent themselves, which beside all the above mentioned factors can as well affect the fluorescence intensity of the probe molecule. It should be noted that a small contribution to the observed decrease in the fluorescence of the guests in the presence of the gray calixarenes could arise simply from the absorption of excitation light by these calixarenes. This could result in a lower total absorption by the

guests, which would result in lower guest fluorescence.

In this work it was found that all fluorescent probes studied with the water-soluble *p*-sulfonic calixarenes showed a decrease in fluorescence upon addition of the calixarenes, presumably due to formation of an inclusion complex. The observation of decreased fluorescence, as opposed to fluorescence enhancement predicted solely by polarity changes upon inclusion, indicates the operation of some specific interactions between the host and guest, providing increased non-radiative decay of the guest. Such interactions could include π-π interactions between the host and aromatic guests. This phenomenon of decreased fluorescence observed could in fact be a result of all of the above mentioned properties of calixarenes. Due to the lack of a dependable supply of quality calixarenes during this project, we were unable to perform the experiments to the level which would provide us with a more reasonable understanding and therefore explanation of this phenomenon.

V. *CONCLUSIONS*

In this project, fluorescence spectroscopy was used to study the supramolecular host properties of cucurbut[7]uril and water soluble sulfonic calixarenes. As results of these studies some useful properties of these compounds as potential supramolecular hosts have been identified.

A significant enhancement of the fluorescence of 2,6-ANS by CB[7], by a factor of 25, was observed in both potassium phosphate buffer and 0.2 M Na_2SO_4 solutions. The excellent fit of the enhancement as a function of CB[7] concentration data in both solvents indicate that simple 1:1 complexation is occurring between the 2,6-ANS guest and CB[7] host, with binding constants of 490 ± 80 M^{-1} and 244 ± 98 M^{-1} , in potassium phosphate buffer and 0.2 M Na_2SO_4, respectively. The lack of a significant blue-shift in the spectrum, in both media, suggests that only the phenyl moiety is inserted into the CB[7] cavity, rather than the naphthalene moiety. If the naphthalene moiety is being included, then a much larger blue shift of the 2,6-ANS spectrum would be expected. The results presented here represent not only the first reported association constant for an inclusion complex of CB[7], but also allow for the direct comparison of the host properties of CB[7] with those of the original cucurbituril, CB[6], since 2,6-ANS as a guest has now been studied. Results suggest that a much stronger complex is formed between 2,6-ANS and CB[7] as compared with CB[6]. Thus, the larger cavity and portal (7.3 Å and 5.4 Å, respectively) of CB[7], makes it a much better size match and host for the 2,6-ANS phenyl ring than CB[6] with the cavity and portal of 5.8 Å and 3.9 Å, respectively, resulting in a much larger fluorescence enhancement

as well as in a much stronger inclusion complex. Thus, CB[7] is seen to have significantly improved host properties over the original cucurbituril, as a result of its more spacious internal cavity.

The results obtained by studying the complexation of 1,8-ANS with CB[7] are very different from those of 2,6-ANS. The maximum fluorescence enhancement of 120 is much larger than that of 25 observed for 2,6-ANS. Also, significant blue shifting of the 1,8-ANS spectrum by 48 nm is observed, while for 2,6-ANS observed blue shift is only 7 nm. Results obtained from the fit of the enhancement as a function of CB[7] concentration data and double reciprocal plot clearly indicate the formation of the higher-order inclusion complexes between 1,8-ANS and CB[7]. In contrast to 2,6-ANS complexation with CB[7], where only phenyl group was included within the CB[7] cavity, results of the complexation of 1,8-ANS with CB[7] indicate the inclusion of the naphthalene moiety into the CB[7] cavity. The major differences in complexation of 2,6-ANS and 1,8-ANS with CB[7] is explained by a consideration of the differing geometry of the two ANS isomers.

Polarity studies showed that the cavity of CB[7] is relatively non-polar, with a cavity polarity similar to a 50:50 methanol:ethanol mixture. Therefore, the observed 1,8-ANS fluorescence enhancement by CB[7] and the significant blue shifting in the spectrum corresponds well with the determined relative cavity polarity. Thus, the ability of CB[7] to enhance the 1,8-ANS fluorescence depends directly on the polarity experienced by 1,8-ANS molecule when incorporated within CB[7] cavity.

In order to determine the thermodynamics of inclusion of 2,6-ANS in CB[7], the association constant K was determined for this host-guest pair at five different temperatures.

It was determined that the more negative ΔG^0 value of formation of CB[7]:2,6-ANS host-guest complex at the lower temperature, 282 K, was mainly a result of a large positive entropy value, and that the decreased ΔG^0 at higher temperatures is mainly a result of a negative entropy value, which opposed the larger negative enthalpy change observed at higher temperatures. Such an observed phenomenon suggests existence of the relationship referred as entropy-enthalpy compensation. This relationship proposes that for host-guest systems in which the enthalpy is quite high, a decrease in entropy is observed as a compensatory mechanism. The van't Hoff plot of lnK versus 1/T for complexation of 2,6-ANS with CB[7] is strongly curved, suggesting temperature dependence of ΔH and ΔS for inclusion,even over this relatively small temperature range used. The curvature in the van't Hoff plot indicates also that there is a change in the total heat capacity, Cp, for the inclusion process. In other words, there is a non-zero ΔCp for this inclusion process.

The time-resolved fluorescence studies showed that the fluorescence decay curve of 2,6-ANS molecule is best described by a two exponential fit decay, indicating that two different types of 1:1 complexes exist. However, equilibrium constants were not able to be obtained from time-resolved fluorescence studies.

The host-guest complexation of water soluble sulfonic calixarenes was also studied by fluorescence spectroscopy. Each probe used in this project showed decreased fluorescence upon addition of the calixarene of interest. Furthermore, addition of these calixarenes to solutions of Dansyl Lysine had a strong effect on the absorption spectrum. A new band was seen to grow and the original Dansyl Lysine band was seen to decrease as a function of added calixarene concentration. The observation of an isosbestic point in the

absorption spectrum indicated the formation of a single type of inclusion complex; however it was not possible to analyze the absorbance data to obtain the value of the association constant for this complex. In studies of lanthanides with these water-soluble calixarenes, fluorescent crystals were obtained. However, it is not clear whether these formed crystals are real host-guest inclusion solids. This general phenomenon of decreased fluorescence observed by studying the inclusion complexes of water soluble sulfonic calixarenes with different probes could be the result of different effects of the calixarenes properties, such as conformation, functionalization of their aromatic rings, structure complexity and their ability to fluoresce, and the interaction of their π electrons with the π electrons of the aromatic fluorescent probes studied. The lack of good quality of available calixarenes for this project prevented the performance of the experiments to the level which would provide a reasonable understanding and therefore the explanation of this phenomenon.

VI. *REFERENCES*

1 Buschmann, H.J.; Jansen, K.; Meschke, C.; Schollmeyer, E. *J. Sol. Chem.* **1998,** *27,* 135-140

2 Meschke, C.; Buschmann, H.J.; Schollmeyer, E. *Thermochim. Acta* **1997,** *297,* 43-48

3 Buschmann, H.J.; Jansen, K.; Meschke, C.; Schollmeyer, E. *Thermochim. Acta* **1998,** *317,* 95-98

4 Kim, J.; Kim, S-J.; Jung, I-S.; Lee, E.; Kang, J-K.; Sakamoto, S.; Yamaguchi, K.; Kim,K. *J. Am. Chem. Soc.* **2000,** *122,* 540-541

5 Berr, P.D.; Gale, P.A.; Smith, D.K. Supramolecular Chemistry, London: Oxford Science Publications 1999

6 Johnston, L.J.; Wagner, B.D. Physical Methods in Supramolecular Chemistry, Vol. 8 of Comprehensive Supramolecular Chemistry, J. Eric D.Davies, John A. Ripmeester, Pergamon Press: Oxford U.K., 1996; Chapter 13

7 O'Connor, D.V.; Philips, D. Time-correlated Single Photon Counting The Royal Institution, London, U.K., Academic Press, London, 1984

8 Lakowicz, J.R. Principles of Fluorescence Spectroscopy Plenum Press, New York and London, 1983

9 Lakowicz, J.R. Topics in Fluorescence Spectroscopy Vol.1, Plenum Press, New York and London, 1991

10 Straughan, B.P,; Walker, S. Spectroscopy, London: Chapman and Hall; New York: Wiley; 1976

11 Reharsky, M.V.; Inoue, Y. *Chem. Rev.* **1998,** *98,* 1875-1917

12 James, D.R.; Siemarczuk, A.; Ware, W.R. *Rev. Sci. Instrum.*, **1992,** *63,* 1170-1175

13 Mock, W.L.; Shih, N.-Y. *J. Am. Chem. Soc.* **1988,** *110,* 4706-4710

14 Cyclodextrins Vol. 3 of Comprehensive Supramolecular Chemistry, Jerry L. Atwood, J. Eric D.Davies, David D. Macnicol, Fritz Vogtle, Pergamon Press: Oxford U.K., 1996

15 Wagner, B.D.; MacRae, A.I. *J. Phys. Chem. B* **1999,** *103,* 10114-10119

16 Mock, W.L.; Shih, N.-Y. *J. Org. Chem.* **1983,** *48,* 3618-3619

17 Mock, W.L.; Shih, N.-Y. *J. Org. Chem.* **1986,** *51,* 4440-4446

18 Buschmann, H.J.; Cleve, E.; Schollmeyer, E. *Inorg. Chim. Acta,* **1992,** *193,* 93-97

19 Buschmann, H.J.; Schollmeyer, E. *J. Incl. Phenom. Mol. Recog. Chem.* **1997,** *29,* 167-174

20 Wagner, B.D.; Fitzpatrick, S.J.; Gill, M.A.; MacRea, A.I; Stojanovic, N. *Can. J. Chem.* **2001,** *79,* 1101-1104

21 Kim, S-T.; Jung, I-S.; Lee, E.; Kim, J.; Sakamato, S.; Yamaguchi, K.; Kim, K. *Angew. Chem. Int. Ed.* **2001,** *40,* 2119-2121

22 Kim, H-J.; Heo, J.; Jeon, W.S.; Lee, E.; Kim, J.; Sakamoto, S.; Yamaguchi, K.; Kim, K. *Angew. Chem. Int. Ed.* **2001,** *40,* 1526-1529

23 Zhang, Y.; Agbaria, R.A.; Warner, I.M. *Supramol. Chem.* **1997,** *8,* 309-318

24 McKervey, A.; Bonmel, V. *Chem. Brit.* **1992,** 724-728

25 Niederl, J. B.; McCoy, J. S. *J. Am. Chem. Soc.* **1943,** *65,* 629

26 Gutsche, D. Calixarene Revisited The Royal Society of Chemistry, Cambridge, 1998

27 Calixarenes as related hosts Vol.2 of Comprehensive Molecular Chemistry, Jerry L. Atwood, J. Eric D.Davies, David D. Macnicol, Fritz Vogtle, Pergamon Press: Oxford U.K., 1996, 103-142

28 Ungaro, R.; Arduini, A.; McGregor, W.; Paganuzzi, D.; Pochini, A.; Secchi, A.; Ugozzoli, F. *J. Chem. Soc. Perkin Trans. 2,* **1996,** 839-846

29 Shinkai, S.; Mori, S.; Koreishi, H.; Tsubaki, T.; Manabe, O. *J. Am. Chem. Soc.* **1986,** *108,* 2409-2416

30 Gutsche, C.D.; Levine, J.A.; Sujeeth, P.K. *J. Org. Chem.* **1985,** *50,* 5802-5806

31 Shinkai, S.; Ohseto, F.; Murakami, H.; Araki, K.; *Tet. Lett.* **1992,** *65,*1217-1220

32 Shinkai, S.; Araki, K.; Tsubaki, T.; Arimura, T.; Manabe, O. *J. Chem. Soc. Perkin Trans. I* **1987,** 2297-2299

33 Arduini, A.; Pochini, A.; Reverberi, S.; Ungaro, R. *J. Chem. Soc. Chem. Commun.* **1984,** 981-985

34 Arimura, T.; Nagasaki, T.; Shinkai, S.; Matsuda, T. *J. Org. Chem.* **1989,** *54,* 3766-3768

35 Shinkai, S.; Mori, S.; Tsubaki, T.; Sone, T.; Manabe, O. *Tet. Lett.* **1984,** *25,* 5315-5318

36 Shinkai, S.; Kawabata, H.; Arimura, T.; Matsuda, T.; Satoh, H.; Manabe, O. *J. Chem. Soc. Perkin Trans. I,* **1989,** 1073-1074

37 Barra, M.; Tao, W. *J. Chem. Soc. Perkin Trans. 2,* **1998,** 1957-1960

38 Liu, Y.; Han, B-H.; Chen, Y-T. J. *Org. Chem.* **2000,** *65,* 6227-6230

39 Wagner, B.D.; Fitzpatrick, S.J. *J. Incl. Phenom. Macro. Chem.* **2000,** *38,* 467-478

40 Wagner, B.D.; MacDonald, P.J. *J. Photochem. Photobiol.* **1998,** *114,* 151-157

41 Time Master Fluorescence Lifetime Spectrometer, Reference Manual, Photon Technology International, **1994**

42 Hamai, S.; Hatamiya, A. *Bull. Chem. Soc. Jpn.* **1996,** *69,* 2469-2476

43 Kosower, E,M.; Dodiuk, H.; Tanizawa, K.; Ottolenghi,M.; Orbach, N. *J. Am. Chem. Soc.* **1975,** *97,* 2167-2178

44 Kosower, E.M.; Dodiuk, H.; Kanety, H. *J. Am. Chem. Soc.* **1978,** *100,* 4179-4188

45 Wagner, B.D.; MacRae, A.I. *J. Phys. Chem. B* **1999,** *103,* 10114-10119

46 Martinez, N.; Junquera, E.; Aicart, E. *Phys. Chem. Chem. Phys.* **1999,** *1,* 4811-4817

47 Gunter, M.J.; Bampos, N.; Jonhstone, K.D.; Sanders, J. K. M. *New. J. Chem.* **2001,** *25,* 166-173

48 Tron, J.R.; Russel, D.; Lewis, E.A.; Murphy, K.P. *Biochem.* **2001,** *40,* 1774-1778

49 Kresheck, G.C. *J. Phys. Chem. B.* **1998,** *102,* 6596-6600

50 Wagner, B. D.; Durber, J. Y. unpublished results.

51 Warner, I.M.; Nelson,G.; Patonay, G. *Analyt. Chem.* **1988,** *60,* 274-279

52 Flamigni,L. *J. Phys. Chem.* **1993,** *97,* 9566-9572

53 Monti, S.; Kohler, G.; Grabner,G. *J. Phys. Chem.* **1993,** 97, 13011-13016

54 Siemiarczuk, A.; Wagner, B.D.; Ware, W.R. *J. Phys. Chem.* **1990,** 94, 1661-1666

55 Ware, W.R.; Wagner, B.D. Chapter 13 in Photochemistry in Organized and Constrained Media, V. Ramamarthy, Ed., 1991

56 Bright, F.V.; Catena, G.C.; Huang, J. *J. Am. Chem. Soc.* **1990,** *112,* 1343-1346

57 Shinkai,S *Tetrahedron,* **1993,** *49,* 8933-8968

58 Liu, Y,; Han, B-H.; Chen, Y-T. *J. Org. Chem.* **2000,** *65,* 6227-6230